

This document is confidential and is proprietary to the American Chemical Society and its authors. Do not copy or disclose without written permission. If you have received this item in error, notify the sender and delete all copies.

From lab to fab: enabling enhanced control of block polymer thin-film nanostructures

Journal:	<i>ACS Applied Polymer Materials</i>
Manuscript ID	ap-2021-00680c.R2
Manuscript Type:	Spotlight on Applications
Date Submitted by the Author:	n/a
Complete List of Authors:	Gottlieb, Eric; University of Delaware, Department of Chemical & Biomolecular Engineering Guliyeva, Aynur; University of Delaware, Department of Chemical & Biomolecular Engineering Epps, Thomas; University of Delaware, Department of Chemical & Biomolecular Engineering

SCHOLARONE™
Manuscripts

1
2
3 **From lab to fab: enabling enhanced control of block polymer thin-film nanostructures**
45 **Eric R. Gottlieb,^{†,§} Aynur Guliyeva,^{†,§} and Thomas H. Epps, III^{*,†,‡,§,#}**
67 [†]Department of Chemical and Biomolecular Engineering, University of Delaware, Newark, Delaware 19716,
8 United States
910 [#]Department of Materials Science and Engineering, University of Delaware, Newark, Delaware 19716, United
11 States
1213 [#]Center for Research in Soft matter and Polymers (CRISP), University of Delaware, Newark, Delaware 19716,
14 United States
1516 [§]Authors contributed equally
1718 *Correspondence to: Thomas H. Epps, III (email: thepps@udel.edu)
1920 **Keywords:** block polymer, self-assembly, thin film, nanomanufacturing, annealing, directed self-
21 assembly
2223 **ABSTRACT:** Block polymer (BP) self-assembly is an ideal approach to generate periodic
24 nanostructures for thin-film applications such as nanolithography, ultrahigh-density memory
25 storage, sensors, and membrane filtration. However, numerous commercial uses require well-
26 ordered nanopatterns and/or precisely controlled domain orientations that can be produced quickly
27 and reliably. In this Spotlight on Applications, advances in BP thin-film fabrication are highlighted
28 including fundamental studies of BP microphase separation, methods to anneal with improved
29 ordering kinetics, and techniques for shear-based directed self-assembly (DSA); the studies
30 discussed represent important steps towards effective large-area manufacturing of nanoscale
31 features. First, combinatorial/gradient and *in situ* investigations of interfacial energetics, solvent
32 interactions, and DSA are presented because of the unique insights they provide with respect to
33 morphology control. Next, methods to manipulate BP thin-film morphologies by annealing or
34 shear-based DSA are discussed, highlighting key aspects for these approaches: speed, adaptability
35 roll-to-roll compatibility, and BP system versatility. Finally, an overview of some of the challenges
36 that limit the wider adoption of BP thin-film technologies, and several opportunities to overcome
37 these hurdles are considered, such as latent alignment and multistep processing.
3839
40 **1. Introduction**
4142 The ability of block polymers (BPs) to self-assemble into well-defined nanostructures has
43 attracted significant research interest for thin-film applications such as nanolithography,^{1, 2}
44 ultrahigh density memory storage,³ sensors,⁴ and membrane filtration.^{5, 6} This attention is driven
45 by the potential for BPs to simplify the production of nanoscale features, as the morphology and
46 size scale of self-assembly can be readily tuned through manipulation of polymer composition,
47 architecture, and overall molecular weight.⁷ The spontaneous nanostructure formation on the basis
48 of molecular interactions is considered a ‘bottom-up’ approach, and it has the potential to be a
49 cost-effective route to overcome many of the limitations of current ‘top-down’ methods.⁸
5051 Established top-down techniques (*e.g.*, photolithography, electron-beam lithography)
52 typically use a mask or a scanning probe to transfer or raster patterns.^{9, 10} These commercially
53 tractable production platforms can fabricate complex features that are effectively defect-free and
54 are extremely important in the industrial manufacturing of electronic components (*e.g.*, integrated
55

circuits) because of the application need for minimal nanostructure flaws.¹⁰ However, several drawbacks of top-down methods include low throughput, poor substrate compatibility, and inherent resolution limitations.¹⁰ Furthermore stringent environmental requirements commonly necessitate the use of clean rooms, which significantly increases processing costs.^{9, 10} These drawbacks have hindered the broader adoption of nanoscale patterns into other types of products and have slowed progress towards higher feature densities in electronics.^{9, 10}

Although there are significant potential benefits to bottom-up approaches, including those that rely on nanostructure generation *via* BPs, the incorporation of such systems in industrial applications has been limited to date.^{9, 10} Perhaps the most notable example of an industrial adoption is IBM's Airgap, which has used a perpendicular-cylinder nanostructure formed by BPs to enable the creation of vacuum gaps between on-chip wires to improve electrical insulation.¹¹ Another application in which BP thin film-derived features have shown promise is magnetic storage media. Researchers at both Western Digital (formerly Hitachi Global Storage Technologies) and Seagate demonstrated the fabrication and performance of bit-patterned media made by BPs with densities greater than 1 Tdot/in².³ However, methods to control BPs for next-generation magnetic storage, lithography, and logic need significant improvement before industrial adoption because of stringent tolerances with respect to features-size variability, line-edge roughness, defect density, etc.^{3, 12} In contrast, the built-in redundancies of dynamic random access memory allow for a defect rate \sim 100x higher than what is acceptable for logic, which makes this use-case a promising entry point for BPs in electronics patterning.¹³

There are additional applications of BP nanostructures that do not have the strict requirements mentioned above, but different challenges have prevented widespread adoption.⁸ For example, membranes for wastewater recovery must be manufactured across orders of magnitude more surface area than circuits,⁶ and although high-performance filtration using BPs has been demonstrated, methods to produce the films with sufficient throughput are lacking.⁵ Scalable fabrication that can produce square meters of BP-based functional nanoporous membranes generally will benefit from continuous processes, such as roll-to-roll (R2R) systems,¹⁴⁻¹⁶ and current BP deposition and alignment approaches are often incompatible with R2R production or too slow for cost-effective manufacturing.⁸

Thus, for broader commercial adoption of BP thin films, patterns need to be formed quickly (*i.e.*, in several minutes or faster), and the processes used must be amenable to integration in production systems for target applications.¹⁷ The requirements of a given purpose dictate which nanoscale characteristics are important to control; common examples include morphology (*e.g.*, spheres, cylinders, lamellae), feature size, grain size, defect density, orientation (parallel or perpendicular relative to the substrate), and in-plane directionality.¹⁷ Although there are strategies to produce nanostructures with a set of chosen attributes, such as substrate modification,^{18, 19} thermal/solvent-based annealing,²⁰ and directed self-assembly (DSA),^{21, 22} existing approaches are limited by the abovementioned drawbacks.⁸ Furthermore, the effectiveness and implementation details of methods to manipulate self-assembly can vary significantly on the basis of the BP used and the nanostructure desired. With an expansive parameter space, it can be a difficult to optimize fabrication protocols to produce a target nanopattern efficiently and consistently, and fundamental studies play an important role in addressing these issues.

The Epps group is tackling these challenges through several investigations that have (1) assessed process conditions *via* combinatorial/gradient screening and (2) probed BP thin-film nanostructure reorganization with *in situ* characterization techniques.^{23, 24} In particular, high-throughput approaches were used to study the complex interplay associated with polymer/substrate

and polymer/solvent interactions. These analyses have elucidated important connections between process conditions and morphology, and they have demonstrated approaches that can be employed to rapidly optimize fabrication procedures. Furthermore, such studies are complementary to other areas of research that are critical to many applications, like the introduction of functionalities into BP-generated nanopatterns (*e.g.*, masks, inorganic replicas, semiconducting blocks, etc.).^{25, 26}

In this Spotlight, we highlight several paths to address the abovementioned challenges, including important contributions from the Epps group (see also **Figure 1**). First, fundamental studies of BP thin-film processing are presented with a focus on understanding the impacts of interfacial effects, annealing, and DSA on morphology. Next, processes to develop or manipulate BP thin-film nanostructures are showcased. Although fundamental studies and process development work synergistically towards the same overarching objective of bringing BPs “from lab to fab”, these workflows have distinct methodologies and specific goals. Finally, ongoing hurdles to the manufacturing of BP thin films, and opportunities to overcome these limitations, are considered.

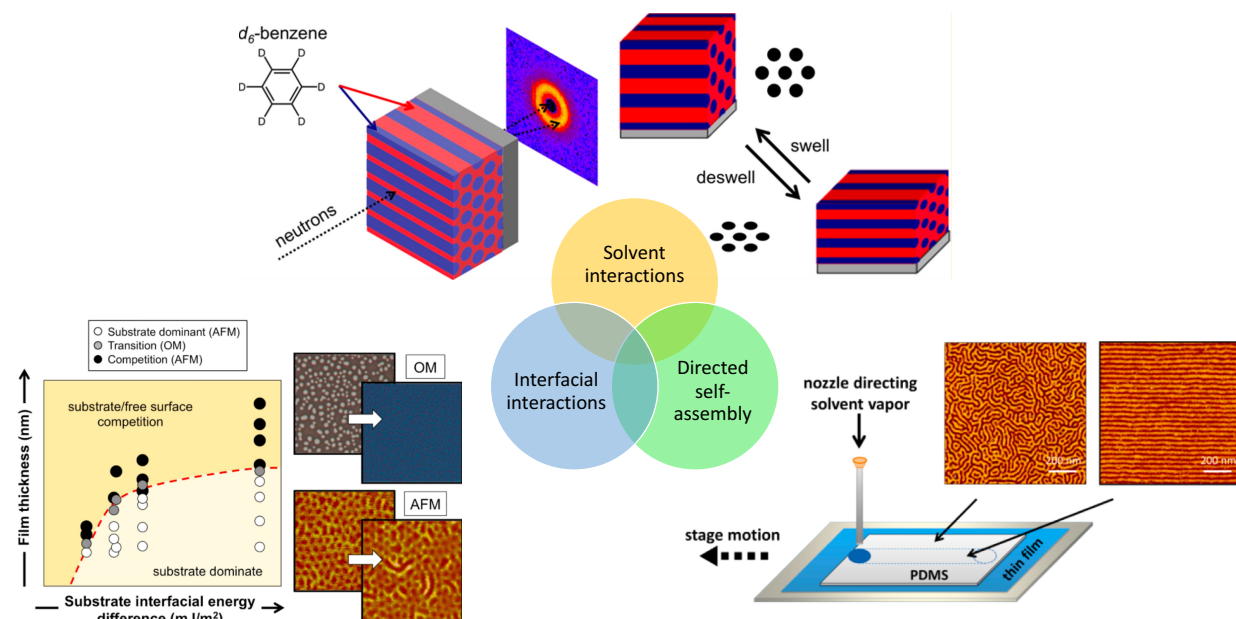


Figure 1. Key aspects of self-assembly and nanostructure control in BP thin films. (Bottom left) The competition between substrate and free surface interfacial interactions is related to film thickness, and the interplay between these factors can impact the surface morphology. Reproduced from ref. 23. Copyright 2016 American Chemical Society. (Top) BPs can reorganize while in a solvent-swollen state; the specific response (*e.g.*, change of number of layers or domain spacing) can vary on the basis of solvent vapor partial pressure and the resulting domain plasticization. Reproduced from ref. 24. Copyright 2016 American Chemical Society. (Bottom right) The application of a shear stress to a BP film can be achieved by solvent vapor to expand and contract an elastomer pad. The solvent vapor also swells the film to provide chain mobility, which can facilitate BP alignment. Reproduced from ref. 22. Copyright 2015 American Chemical Society.

2. Studies of BP Thin-Film Self-Assembly Processes

BP self-assembly is a multifaceted process that becomes more complex when the polymers are confined to thin-film geometries. The impacts of competing forces can be difficult to deconvolute, and large parameter spaces are challenging to investigate systematically. For example, preferential interactions between a polymer block and the substrate can influence the nanostructure formed, but the magnitude of this effect is not constant through the thickness of the film.^{18, 23} As such, *in situ* and gradient/combinatorial analyses are critical to determine underlying mechanisms of self-assembly and to optimize process parameters to improve final nanostructures.^{18, 27, 28} In this section, several studies are described that use these tools to probe the morphological effects of interfacial interactions, solvent energetics, and DSA.

2.1 Interfacial Interactions

In a thin-film configuration, surface/interface energy is a driving factor for the orientation (parallel or perpendicular) of BP nanostructures. For example, in the simplest case of an AB diblock polymer on a solid substrate, interactions between one block and the substrate can direct self-assembly to form patterns that are in-plane or out-of-plane relative to the surface.^{29, 30} Nanostructure orientation is critical for many applications (*e.g.*, perpendicular cylinders for nanofiltration), but robust control over this aspect of self-assembly is not easy to achieve — block chemistries, substrate chemistry, the free surface, and film thickness all have interdependent effects on nanopattern orientation. Often, nanostructures perpendicular to the substrate are desirable, but to achieve this result, both blocks are normally expected to have similar surface energies at the polymer/substrate and polymer/air interfaces.¹⁹ Thus, researchers have studied approaches to modify surface energies through substrate surface manipulation and/or the introduction of new layers, such as topcoats to tune interactions at the polymer/air interface.³¹

Substrate modification is one promising route to control surface chemistry. Techniques can use crosslinkable random copolymers,³² hydroxyl-terminated homopolymers,³³ or polymer grafts on the substrate.^{19, 29, 34} For example, chlorosilanes can react with native oxide surfaces of silicon to form a monolayer that modifies surface energy.^{18, 19, 34} Different surface chemistries can be generated from various chlorosilane chemistries (*e.g.*, benzylidimethylchlorosilane [benzyl silane] or *n*-butyldimethylchlorosilane [*n*-butyl silane]), and a wide range of interactions, both preferential or nonpreferential, can be obtained. Furthermore, blends of organosilanes with different functionalities can be used to fine-tune surface energy, which adds granularity to the accessible parameter space.¹⁸ These mixtures also can vary spatially — Julthongpiput *et al.* demonstrated a route to form micropattern surface gradients by varied UV-ozone exposure, which chemically modifies a hydrophobic chlorosilane slowly with the incorporation of oxygen-containing groups.³⁵

The Epps group has employed modified surfaces with gradients between two distinct chlorosilanes to enable high-throughput investigations of the effects of surface energies on polymer nanostructures.^{19, 34} One key approach involved cross-deposition onto a substrate of two chlorosilanes under dynamic vacuum with the ability to tune gradient profiles and surface energies imparted through control parameters such as reservoir size and position.³⁴ The surfaces produced by this process enabled one to efficiently probe a series of interfacial interactions using a single polymer film.

This framework, in conjunction with gradient thickness films, was employed by the Epps group to assess the self-assembly of poly(styrene-*b*-isoprene-*b*-styrene) (SIS) across a wide range

of film thicknesses and substrate chemistries.¹⁸ Gradient-thicknesses films were used to demonstrate that preferential interactions between the polystyrene blocks and either bare silicon or benzyl silane led to the formation of parallel cylinders independent of the film thickness.¹⁸ In contrast, preferential interactions between the polyisoprene block and *n*-butyl silane led to the formation of distinct nanostructures as a function of film thickness.¹⁸ The films exhibited a mixture of parallel cylinders and hexagonally perforated lamellae (HPL) across most thicknesses, with HPL exclusively present only at narrow thickness ranges of $t = 89\text{--}91\text{ nm}$ ($3.30d\text{--}3.37d$, d is interlayer spacing and had a value of 27 nm for this system) and $t = 116\text{ nm}$ ($4.30d$).¹⁸ The difference in thickness between these HPL-exclusive regions was $\sim 27\text{ nm}$, which matches the interlayer spacing for the polymer thin film.¹⁸ Films cast onto gradient benzyl silane to *n*-butyl silane surfaces exhibited gradual morphological transitions from parallel cylinders to HPL with mixed states at intermediate compositions (**Figure 2a**).¹⁸ These high-throughput gradient techniques expedited the identification of both the surface chemistry/energy and film thickness windows that produce parallel cylinders, HPL, and mixtures of the two nanostructures. Importantly, this combinatorial approach to fabricate film thickness and monolayer surface chemistry gradients is a powerful screening tool to probe new materials and identify conditions to obtain desired morphologies.

With the many possible combinations of surface modifications and polymer blocks, a method to predict nanostructure orientation on the basis of key substrate/polymer interactions could aid in the design of thin-film systems through the reduction of extensive parameter space exploration. Such an approach was reported by the Epps group whereby the effects of total, dispersive, and polar substrate surface energy components of thin-film self-assembly were studied systematically and quantitatively.³⁶ This framework can be used to match the desired BP thin-film nanostructure with chemically modified substrates. Poly(methyl methacrylate-*b*-*n*-butyl acrylate) (PMMA-PnBA) films with gradient thicknesses were cast onto substrates with different surface chemistries and thermally annealed, and the wetting behavior was characterized by their island/hole structures measured by *in situ* or *ex situ* optical microscopy.³⁶ This rapid screening approach leveraged the fact that symmetric and asymmetric wetting of diblock polymers (*i.e.*, whether the same or different polymer blocks will wet substrate and free surface) are commensurate at integer and half-integer domain lengths, respectively, and films can form terraces at other thicknesses.³⁶ The results indicated that wetting behavior was driven by repulsive total surface energy whereas through-film interactions were influenced by the attractive pieces of the dispersive and polar components.³⁶

The impact of polymer/substrate interactions propagates through films, but the magnitude of this effect decreases with an increase in film thickness, which can lead to differences in nanostructure orientation at different depths.²³ Because many applications require uniform nanoscale features through films, the Epps group studied the thickness dependence of interfacial interactions on surface morphology.²³ The competition between polymer/substrate and polymer/free surface for PMMA-PnBA was investigated by a similar approach to what was described above.²³ Because preferential wetting leads to island/hole formation at incommensurate film thicknesses, the disappearance of these features indicated a transition from substrate dominant to substrate/free surface competition (*i.e.*, critical propagation depth) (**Figure 2b**).³⁷ This critical propagation depth was mapped as a function of the interfacial energy difference between the substrate and polymer blocks — the critical propagation depth increased linearly at small interfacial energy differences before plateauing at larger interfacial energy differences.²³ Specifically, long-range decoupled surface energy components were predictive of critical

propagation depth, which can help in the design of systems with uniform through-film nanostructures for applications such as nanolithography, nanotemplating, and nanoporous membranes.²³ This propagation depth-based limitation of substrate modification also points to the need to combine approaches, such as substrate surface modification with topcoats, to reliably produce high-aspect-ratio films.³¹

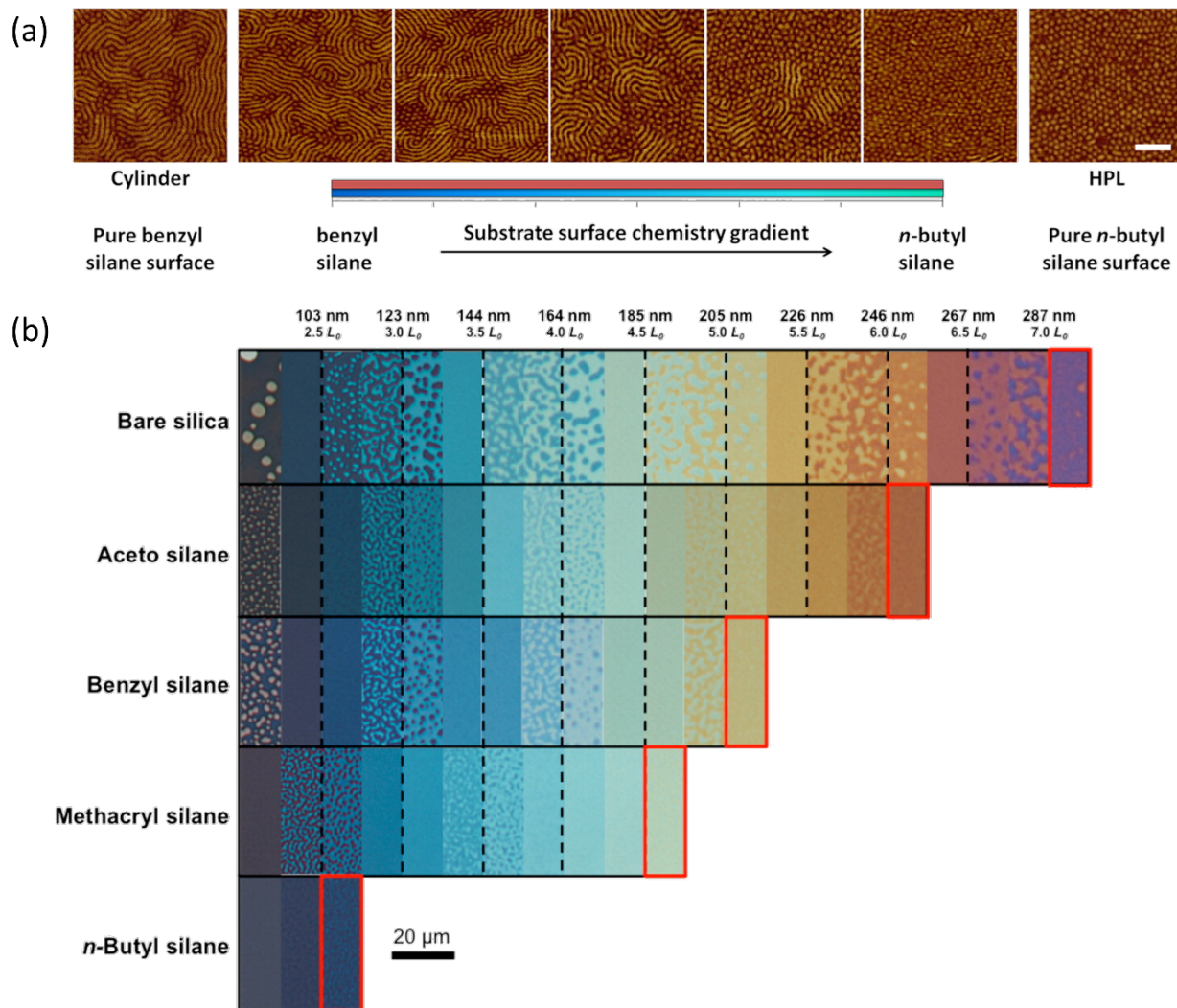


Figure 2. Polymer/substrate interactions. (a) Atomic force microscopy (AFM) phase images of a thermally annealed SIS film cast onto a gradient monolayer. Parallel cylinders were found near the benzyl silane end with a transition to HPL as the *n*-butyl silane composition on the substrate increased. The scale bar represents 200 nm and applies to all images. Reproduced from ref. 18. Copyright 2013 American Chemical Society. (b) Composite optical microscopy images of gradient thickness PMMA-PnBA films on various substrates. Island/hole structures were formed at integer or half integer domain spacings for asymmetric (bare silica, aceto silane, benzyl silane) and symmetric (methacryl silane, *n*-butyl silane) wetting substrates, respectively. The red boxes correspond to critical film thicknesses at which island/hole formations were expected but not present, which indicates a transition from a substrate dominant to a substrate/free surface

competition regime. The scale bar applies to all micrographs. Reproduced from ref. 23. Copyright 2016 American Chemical Society.

2.2 Solvent Interactions

The interactions between polymers and solvents also are important driving forces in self-assembly. Polymer thin films are typically coated from a dilute polymer solution, and the choice of casting solvent can significantly impact the initial (and final) nanoscale morphology.³⁸ After a film is cast, the reintroduction of solvent can plasticize the polymer to enable further coarsening of the self-assembled structure and manipulation of the BP phase behavior — the nanostructure is sensitive to many factors, such as solvent/block compatibility, swelling ratio, and solvent removal rate.^{20, 39} For example, mixtures of solvents can be used to anneal polymers to target a desired morphology on the basis of selective swelling of a block.⁴⁰⁻⁴² Yet, the mechanisms of nanostructure reorganization in these systems need to be understood to improve annealing processes.

BP thin films in solvent-swollen states self-assemble to minimize energy, but the nanostructures formed do not necessarily represent energetic minima of the final unswollen films. In these instances, solvent removal can have a strong impact on the final morphology due to kinetic trapping. Kim *et al.* first reported these effects with poly(styrene-*b*-butadiene-*b*-styrene) films whereby casting solvent evaporation rates were varied.⁴³ Fast evaporation led to poorly ordered films, and successively slower solvent removal formed nanostructures that transitioned from perpendicular cylinders, to perpendicular/parallel mixed orientation cylinders, to parallel cylinders.^{43, 44} The Epps group studied the effect of deswelling rate from solvent vapor annealing (SVA) on morphology with SIS — solvent-swollen BPs were deswelled at different rates, and the through-film morphologies were probed at key points of the solvent removal process.³⁹ Well-controlled UV-ozone etching combined with AFM imaging of quenched films allow the group to probe morphology and orientation as a function of depth.³⁹ The orientation of SIS thin films varied on the basis of solvent removal rates, with the formation of perpendicular cylinders for films deswelled slowly and parallel cylinders for more highly quenched systems.³⁹ The through-film morphologies of films kinetically trapped at different stages of deswelling suggested that the mechanism of cylinder reorientation propagated from the free surface to the substrate.³⁹ These results demonstrate how rate of solvent removal can be an important parameter for the manipulation of BP nanostructures.

Another useful approach to control morphology is through selective-solvent swelling and SVA by multiple solvents. As with the combinations of chlorosilanes described in the previous section, an expansive parameter space can make it labor intensive to target a desired nanostructure. To investigate the impact of solvent mixtures on morphology efficiently, a gradient technique was developed by the Epps group that employs a microfluidic mixing tree.⁴² In this system, two solvent vapor streams were fed into separate inlets.⁴² At each stage of the tree, mixing occurred to produce various ratios of each solvent in a channel, in which a film is annealed.⁴² This approach was used to probe the effects of *n*-hexane and tetrahydrofuran on SIS: the *n*-hexane is preferential to the polyisoprene block and a poor solvent for the polystyrene block, and tetrahydrofuran is a good solvent for both blocks, with a slight preference for the polystyrene block.⁴² The SIS exhibited either a spherical morphology or perpendicular cylinders when annealed by pure *n*-hexane vapor, and the films transitioned to parallel cylinders upon annealing from a vapor mixture richer in tetrahydrofuran.⁴² The formation of spheres would occur on the basis of an increased volume fraction of the polyisoprene block with *n*-hexane, whereas perpendicular cylinders might have

1
2
3 formed to maximize the exposure of the polyisoprene block to the surface due to its position as the
4 midblock in a triblock system. Microfluidic mixing trees enable high-throughput screening of
5 solvent ratios for the identification of microstructures and morphology transformations of interest
6 through efficient optimization of SVA parameters.
7

8 Fundamental studies of solvent/polymer interaction are essential for understanding self-
9 assembly processes.^{45, 46} Experimental connections between the swollen- and dried-film
10 nanostructures are nontrivial because of the difficulty associated with performing *in situ*
11 measurements on films in a swollen state. However, carefully designed experiments that employ
12 electron microscopy, grazing incidence small-angle X-ray scattering, neutron scattering,
13 spectroscopic ellipsometry, or AFM can probe the swollen films *in situ*.^{24, 28, 45, 47-49} For example,
14 environmentally controlled AFM can be used to examine the *in situ* swelling of BP thin films.
15 With this method, direct investigation of swelling kinetics at the limit of single-layer polymer films
16 was possible.⁴⁷ Separately, an *in situ* study from the Epps group elucidated the importance of
17 polymer/solvent interactions on morphology development through a combination of small-angle
18 neutron scattering (SANS) (in-plane features) and neutron reflectivity (out-of-plane features).²⁴
19 Neutron scattering with selective deuteration can enable higher polymer/polymer and
20 polymer/solvent contrast in comparison to X-ray scattering.²⁴ Solvent (d₆-benzene) distributions
21 in the block domains of SIS were tracked at different solvent partial pressures, and solvent
22 distribution profiles were obtained *via* SANS and neutron reflectivity (**Figure 3a**).²⁴ These
23 distribution profiles were used to determine domain size, number of layers, and film thickness for
24 the different states, and Flory-Huggins polymer-solvent interactions ($\chi_{\text{poly-sol}}$) were ascertained on
25 the basis of preferential segregation of solvent into the polystyrene phase.²⁴ Solvent removal and
26 film response occurred in two distinct stages, distinguished on the basis of the effective glass
27 transition temperature (T_g) of polystyrene: if the T_g of polystyrene was below room temperature,
28 the number of cylinder layers changed to accommodate changes in film thickness; if the T_g of
29 polystyrene was above room temperature, domain spacing changed in response to variations in
30 film thickness.²⁴ These *in situ* neutron-based methods enabled unique insights into the effects of
31 polymer/solvent interactions on nanostructure reorganization.
32
33
34
35

36
37
38
39
40
41
42
43
44
45
46
47
48
49
50
51
52
53
54
55
56
57
58
59
60

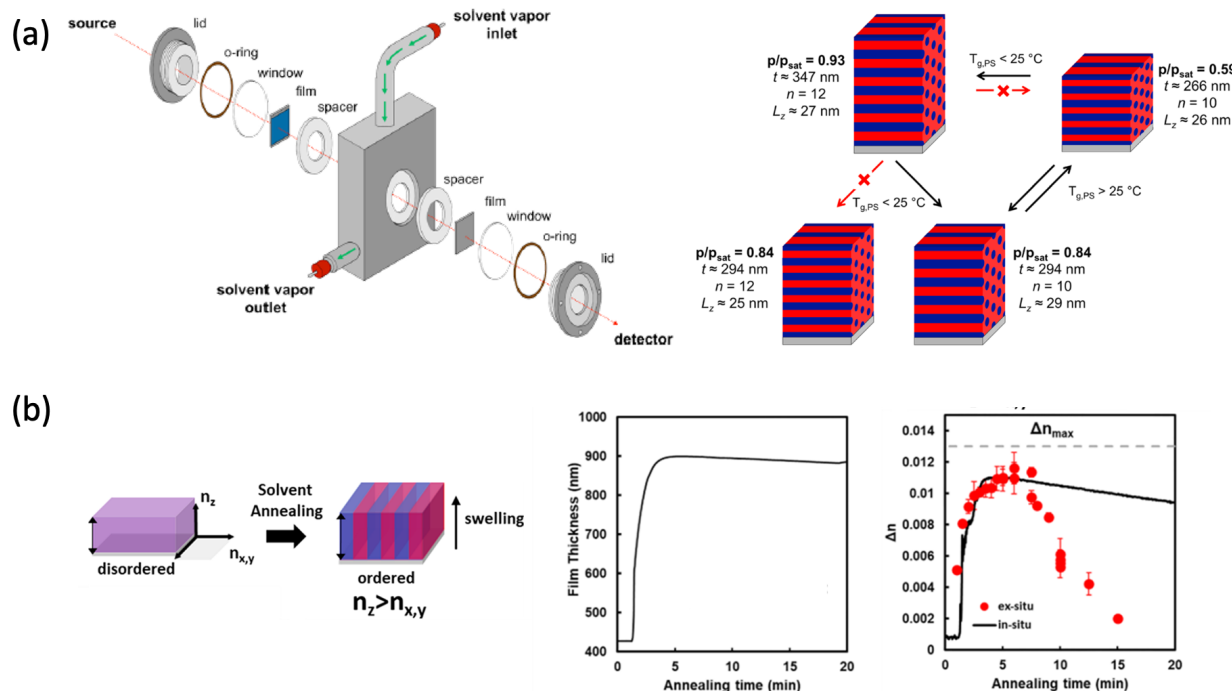


Figure 3. *In situ* studies by SANS and spectroscopic ellipsometry on BP thin films. (a) Schematic of a sample cell for *in situ* SANS measurements with SVA, and an illustration of the different morphological changes the polymer layers went through during swelling and deswelling on the basis of the environmental conditions. Reproduced from ref. 24. Copyright 2016 American Chemical Society. (b) Kinetic monitoring of poly(styrene-*b*-2-vinylpyridine) thin-film self-assembly by *in situ* spectroscopic ellipsometry with chloroform vapor at a steady vapor pressure. Film thickness (left), *in situ* birefringence ($\Delta n = n_z - n_{x,y}$) (right, black line), and *ex situ* birefringence (red circles) data as a function of annealing time. Although birefringence correlated with film thickness initially, *ex situ* birefringence measurements deviated with longer annealing times. Reproduced from ref. 28. Copyright 2020 American Chemical Society.

Another efficient tactic to study kinetic pathways of BP films during SVA uses spectroscopic ellipsometry to assess domain formation on the basis of optical birefringence (**Figure 3b**).²⁸ Fakhraai and coworkers employed this approach to investigate self-assembly of cylinder- and lamellae-forming BP films.²⁸ Isotropic or uniaxial anisotropic models were used to fit *ex situ* ellipsometry data for perpendicular-cylinder- and perpendicular-lamellae-forming BP films annealed for different amounts of time, and the birefringence values obtained were correlated with autocorrelation function values of the nearest neighbor distance calculated from AFM images.²⁸ The same BP annealing then was probed by spectral ellipsometry *in situ*;²⁸ the BP films formed ordered domains that were stable in the swollen state but disorder with rapid drying.²⁸ The authors noted that *in situ* and *ex situ* spectral ellipsometry yielded different birefringence values, suggesting that the nanostructures of the solvent-swollen films changed when quenched.²⁸ As such, spectral ellipsometry enables one to decouple BP self-assembly and loss of order that occurs during solvent annealing and solvent evaporation, which is difficult to probe by other, slower techniques.²⁸

2.3 Directed Self-Assembly

DSA techniques employ external drivers, such as surface effects (*i.e.*, graphoepitaxy or chemical epitaxy)^{17, 50} or applied forces (*i.e.*, electric, magnetic, or shear),⁵¹⁻⁵³ to bias self-assembly, and these methods can be used to form nanostructures with long-range order or improve ordering kinetics in comparison to conventional (isotropic) annealing.²¹ These approaches often combine an environment that increases chain mobility (*e.g.*, heat or solvent) with a topological pattern, a chemical pattern, or a field.^{51, 52, 54-57} DSA has additional tunable handles for optimization, such as field strength, and the self-assembly pathways that BPs undergo may differ on the basis of the type of DSA used. As such, gradient and *in situ* investigations are critical to understand the underlying mechanisms of these methods and to improve their efficiency in manufacturing-related applications.^{58, 59}

Scattering methods are often employed for mechanistic *in situ* studies of self-assembly because they can probe samples nondestructively that are subjected to external stimuli.^{24, 27, 45, 60} For example, Osuji and coworkers investigated the order-disorder transition and alignment dynamics of a liquid-crystalline BP in bulk and thin films under high magnetic fields by *in situ* small-angle X-ray scattering.⁶⁰ Temperature- and time-resolved measurements unlocked important mechanistic insights into the rearrangement process of liquid-crystalline BPs — no measurable field-induced shift in the order-disorder transition temperature (T_{ODT}) was found, which indicates that selective melting was not a factor in the system's response to magnetic fields.⁶⁰ Instead, alignment occurred by slow grain rotation in the mesophases.⁶⁰ It is important to note that the structural data collected by *in situ* small-angle X-ray scattering during the rearrangement process were critical, as the conclusions drawn were not readily obtainable by measurements on samples before and after alignment.

Although magnetic fields can effectively orient certain systems, shear alignment also has been a promising approach because it has both been adapted to work with a number of annealing techniques and tested on many polymer systems.^{22, 41, 61, 62} Typically, an elastomeric pad is placed on top of the BP thin film to transfer shear force that can be produced by two primary mechanisms: lateral displacement or expansion/contraction.^{51, 52, 54, 55, 63} In general, the former employs heat and a weight on top of the elastomer that is displaced laterally,⁵⁴⁻⁵⁶ and the latter involves solvent swelling/deswelling or heating/cooling to induce expansion and contraction of the pad.^{51, 52, 57} To probe the relationship between shear strength and orientation quality for poly(styrene-*b*-*n*-hexyl methacrylate) thin films, Davis *et al.* used an experimental setup that applied a shear gradient as opposed to a single shear stress (**Figure 4a**).⁶³ Polydimethylsiloxane (PDMS) oil replaced the crosslinked elastomer, and a parallel plate rheometer produced shear stress gradients as a function of radial distance from the center of the film.⁶³ The setup enabled rapid assessments of the relationship between shear and alignment quality for several parameters. The critical stress needed to induce alignment increased linearly with overall molecular weight and the weight fraction of the cylinder-forming block, and the critical stress decreased with increasing film thickness.⁶³ Furthermore, with the exception of film thickness, conditions that yielded lower critical stresses had faster (*i.e.*, smaller) rate constants.⁶³ These results provided important insights into the relationships between operating parameters and alignment quality/kinetics.

Shear alignment is difficult to investigate *in situ* because the PDMS pad placed on top of the film interferes with data acquisition for measurements such as X-ray scattering, scanning electron microscopy, and AFM. The relative thickness of the elastomer needed to shear films obscures surface features of the film underneath from effective scanning electron microscopy or AFM imaging. Furthermore, although X-ray scattering techniques are effective for assessing

nanoscale periodicity, the electron density-based contrast mechanism is problematic for investigating a polymer under a silicon-containing material.²⁷ Neutron scattering, on the other hand, has a different contrast mechanism and therefore can probe samples with similar elemental compositions through selective deuteration.²⁷ The Epps group used an approach to identify the kinetic pathways between disordered and ordered states of BP thin films subjected to these forces that was similar to the *in situ* SANS studies employed to investigated SVA with soft shear (SVA-SS).²⁷ To overcome the large diffuse scattering contribution (background) from PDMS pads that apply the shear stress, the polystyrene blocks of the SIS were deuterated, which enhanced contrast with the polyisoprene block. SANS patterns were collected at different stages of SVA-SS swelling and deswelling (Figure 4b).²⁷ For SVA-SS, the reduced intensity of the primary scattering peak suggested a combination of solvent swelling and shear stress promoted chain mixing and disorder, and removal of solvent precipitated the formation of small, aligned grains.²⁷ During SVA, a similar drop was not noted, which indicated that the level of solvent swelling was not sufficient to disorder the film on its own.²⁷ Note, this mechanism was different than the slow grain rotations shown by Osuji *et al.* of liquid-crystalline BPs under strong magnetic fields.⁶⁰ As with the *in situ* small-angle X-ray scattering study, these insights into the intermediate nanostructures of BP systems were not possible from simply measuring the samples after they underwent rearrangements.

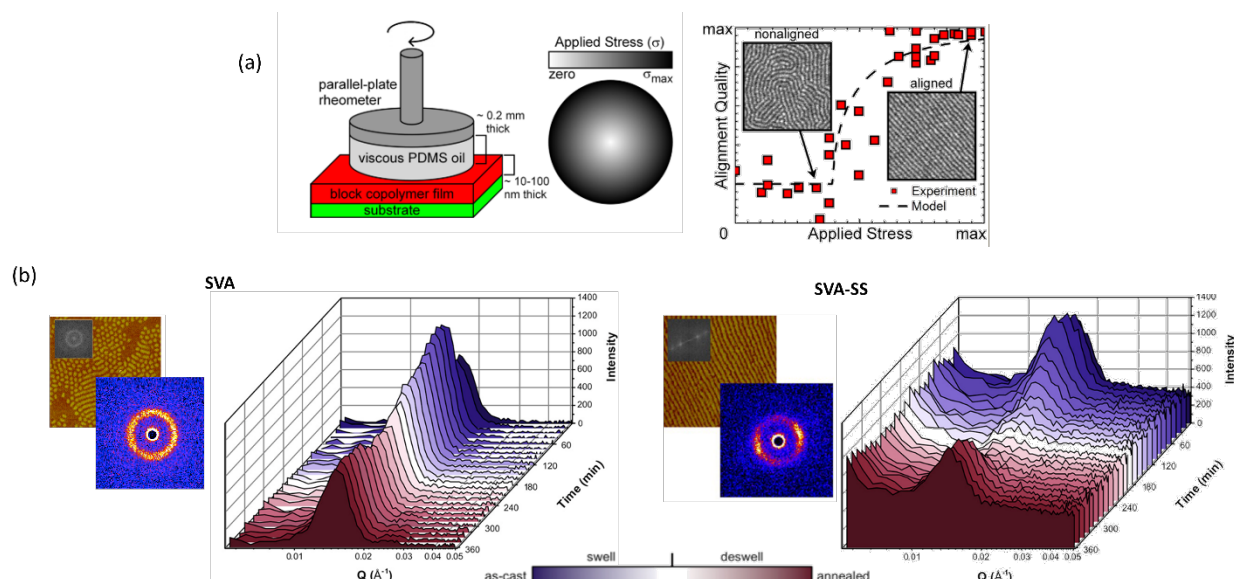


Figure 4. Studies of shear-based DSA. (a) Schematic of an experimental setup to generate shear-stress gradients, a top-down view of the applied stress gradient, and a curve of alignment quality as a function of applied shear stress for a BP system. Reproduced from ref. 63. Copyright 2015 American Chemical Society. (b) A representative SANS pattern, corresponding AFM phase image, and *in situ* SANS temporal data for poly(deuterated styrene-*b*-isoprene-*b*-deuterated styrene) over the course of swelling and deswelling for SVA (left) and SVA-SS (right). Adapted from ref. 27. Copyright 2017 American Chemical Society.

3. Methods to Manipulate Nanostructure

Fundamental studies of BP self-assembly provide an important framework to understand how nanostructures develop when subjected to different conditions, and the conclusions drawn from such studies aid researchers in the creation of new techniques that overcome practical challenges associated with the translation to application. Methods to develop or control BP nanostructures should be compatible with other steps in manufacturing processes and function with polymer systems that are representative of the materials needed for a given industrial application. For example, many of the most common routes to anneal polymer thin films in a laboratory environment (e.g., thermal annealing and SVA)^{20, 64} are limited to batch-mode operation, and ordering kinetics are often slower for systems of potential interest, such as high- χ or ultrahigh molecular weight (UHMW) BPs.^{65, 66} In this section, several methods for annealing and DSA are discussed, and notable features are highlighted, such as amenability to continuous operation, enhanced ordering kinetics, or demonstrated effectiveness for difficult-to-process polymer systems. Also, because these approaches are assessed on the basis of defect densities and long-range order, it is critical to have consistent metrics for comparison, along with accessible tools to carry out the requisite analyses.¹²

3.1 Annealing Methods — Enhanced Ordering Kinetics and Roll-to-Roll Compatibility

BP films cast from fast-evaporating solvents typically have nanostructures that are trapped in quenched, nonequilibrium morphologies with poor phase separation.²⁰ Higher-order BP thin-film nanostructures can be developed by creating an environment that enables rearrangement *via* heat or plasticization of polymer chains to lower their energy states.²⁰ Thermal annealing and SVA are the most established examples. In the case of thermal annealing, BPs are heated above the T_g s of both blocks, whereas in SVA, BPs are swollen with solvent to lower the T_g s to below the ambient temperature.²⁰ Although thermal annealing and SVA can produce well-ordered nanostructures, their utility in manufacturing is currently limited by long processing times, lack of spatial control, and incompatibility with R2R processing.⁶⁷ Furthermore, these methods are typically limited to batch-mode operation because they usually involve placing samples in enclosures so that either heat can be applied under vacuum or a solvent-rich vapor atmosphere can be maintained.⁶⁸ Over the years, adaptations to these techniques have been developed to overcome the abovementioned limitations with faster ordering kinetics and/or R2R compatibility (**Table 1**).

Table 1. Key characteristics of various annealing methods

Method	Advantages	Disadvantages	References
Thermal annealing	Well-established, capable of producing low defect-density films	Slow (hours or days), limited to batch-mode operation, nonideal for thermally sensitive polymers	⁶⁴
Solvent vapor annealing (SVA)	Capable of selective block swelling, compatible with most polymers	Slow (hours), difficult to control, limited to batch-mode operation	²⁰
Raster solvent vapor annealing (RSVA)	Spatially controllable, fast in comparison to SVA (100 $\mu\text{m/s}$ linear speed), easier to control than SVA, compatible with most	Limited with respect to sharpness of the transition between annealed and unannealed regions	⁶⁹

	polymers, adaptable to continuous operation		
Cold zone annealing (CZA)	Adaptable to continuous operation	Nonideal for thermally sensitive polymers, slow (10 $\mu\text{m/s}$ linear speed)	⁷⁰
Hot zone annealing (HZA)	Capable of producing millimeter-sized grains	Nonideal for thermally sensitive polymers or polymers unstable above their T_{ODT} , slow (2 mm/day)	⁷¹
Laser zone annealing (LZA)	Fast (linear process speeds ~1 mm/s)	Nonideal for thermally sensitive polymers, limited to batch-mode operation due to vacuum requirements, restricted to light absorbing substrates	⁷²
Direct immersion annealing (DIA)	Adaptable to continuous operation, easier to control than SVA	Slow (hours), difficult to design DIA systems that balance good and bad solvents for effective annealing	⁷³
Nonvolatile solvent annealing	Adaptable to continuous operation, fast in comparison to SVA	Required to use alternative means of solvent removal as opposed to evaporation	⁷⁴
Low molecular weight homopolymer assisted annealing	Effective for annealing UHMW BPs	Specialized for UHMW BPs, limited by disadvantages of SVA and/or thermal annealing	⁶⁶

‘Zone’ methods, which use localized stimuli to anneal films, have a number of benefits over simply exposing films to higher temperature or solvent vapor. Thermally-driven zone methods, such as hot zone annealing (HZA), cold zone annealing (CZA), and laser zone annealing (LZA) involve the application of concentrated thermal energy either with a hot wire sandwiched between cold blocks or photothermally *via* a laser.^{68, 70, 71, 75, 76} Beyond the mode of heat delivery, the main differences between these techniques come from the maximum temperature applied relative to the BP’s T_{ODT} and the sharpness of the thermal gradient — HZA heats a BP above its T_{ODT} ; CZA heats a BP above the T_g s of both blocks but below the T_{ODT} with thermal gradients of $\nabla T \sim 14 - 45 \text{ }^\circ\text{C/mm}$; LZA heats to temperatures as high as 500 $^\circ\text{C}$ but for very short durations because thermal gradients can reach $\nabla T \sim 4000 \text{ }^\circ\text{C/mm}$.^{70, 76, 77} The residence times for (photo)thermal zone annealing are much shorter than those of conventional thermal annealing to achieve the same degree of order, which implies that the temperature gradients can increase the ordering kinetics for heat-based nanostructure development.⁷⁷ However, there are still significant challenges with these methods — polymer compatibility with (photo)thermal techniques can be limited by lack thermal stability. Furthermore, although CZA is the only approach to be tested in a true R2R system, it operated at velocities of $\sim 10 \mu\text{m/s}$;⁷⁸ in contrast, LZA can be employed at speeds on the order of 1 mm/s, but it requires a vacuum chamber and is typically constrained to substrates capable of the necessary light absorption (*e.g.*, doped Si wafers,^{61, 79} graphene,⁸⁰ or germanium coatings⁷²) (**Figure 5a**).

Another category of zone annealing involves focused solvent vapor, as opposed to heat, to develop the BP nanostructure. One method from the Epps group, raster solvent vapor annealing (RSVA), uses a nozzle to localize a solvent-rich vapor stream to a desired annealing zone (**Figure**

5b).⁶⁹ RSVA can develop BP nanostructures with raster speeds up to $\sim 100 \mu\text{m/s}$, and the ordering kinetics are significantly faster than conventional SVA.⁶⁹ Additional advantages of solvent-based zone annealing over thermal-based zone annealing include broader compatibility with temperature-sensitive polymers and increased tunability with respect to the ultimate morphology and orientation through solvent choice.

Thermal annealing and SVA also have been successfully combined through approaches such as solvothermal annealing⁸¹ and warm-solvent annealing.⁸² Despite reports of successful hybrid strategies to effectively develop BP nanostructures, there are limited instances of extending this tactic to zone-based methods. One such example from Singer *et al.* used focused laser spike zone annealing in combination with solvent vapor exposure to increase the polymer chain mobility and possibly provide other synergistic ordering effects such as thermocapillary shear.⁷⁹ With many other techniques for zone-based annealing, there is a significant opportunity to further improve nanostructure control and ordering kinetics with these types of hybrid approaches.

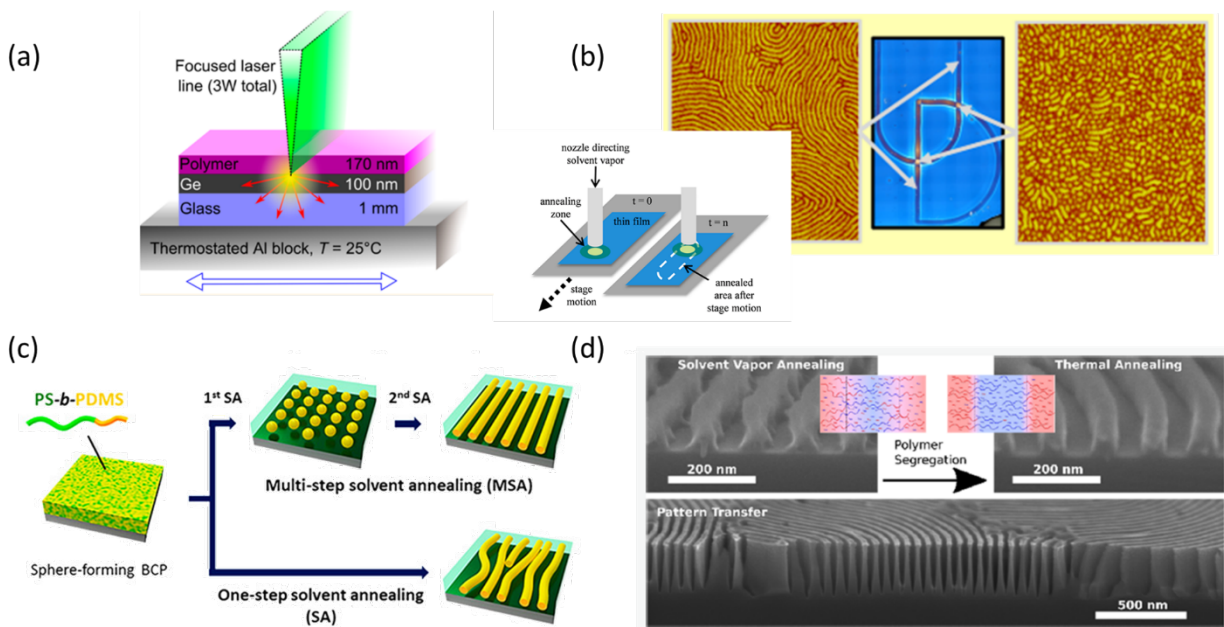


Figure 5. (a) Schematic representation of LZA: light is absorbed by a layer of germanium under a BP thin film to induce heating (yellow). The thermal profile is determined by the laser line and conduction (red arrows). Reproduced from ref. 72. Copyright 2015 American Chemical Society. (b) Illustration of the RSVA process and AFM images of an SIS thin film after a single pass of RSVA. Adapted from ref. 22. Copyright 2012 American Chemical Society. (c) A process for rapid formation of well-ordered line patterns through morphological transitions, and production of core-shell line structure using multi-step solvent annealing. Reproduced from ref. 65. Copyright 2019 American Chemical Society. (d) Annealing of UHMW BPs with low molecular weight homopolymers and SVA, and corresponding cross-sectional scanning electron microscopy images of a UHMW poly(styrene-*b*-methyl methacrylate) after self-assembly. Reproduced from ref. 66. Copyright 2020 American Chemical Society.

Often, the BPs used for studies span a limited range of molecular weights and χ values, and systems that deviate strongly from classical self-assembly process (e.g., by having high χ values

1
2
3 or ultrahigh molecular weights, $M_n > 5 \times 10^5$ g/mol) pose significant challenges to effective
4 nanostructure development.^{83, 84} In the case of high- χ BPs, the stronger segregation between blocks
5 necessitates longer annealing times, often greater than 12 h for SVA.⁶⁵ Careful manipulation of
6 the BP's nanostructure during annealing and the use of multiple annealing steps can be an effective
7 route to reduce processing time and/or produce non-standard patterns for these systems.⁶⁵ Those
8 improvements are enabled by two key benefits of SVA as an annealing method: first, chain
9 mobility has a stronger dependence on solvent swelling than to temperature, which can make SVA
10 a faster route to achieve the same degree of order; second, selective swelling of blocks enables the
11 manipulation of BP volume fractions and thus morphologies.⁸⁵ The ability to tune BP volume
12 fractions without synthesizing a new copolymer can be leveraged to produce a desired pattern
13 quickly and with low defect densities by adjusting the nanostructure across multiple steps. For
14 example, Choi *et al.* showed that an aligned cylindrical morphology could be achieved more
15 quickly from an intermediate spherical nanostructure as opposed to annealing to produce the
16 desired structure from the start (**Figure 5c**).⁶⁵ This result was demonstrated with a poly(styrene-*b*-
17 dimethylsiloxane) thin film that was first annealed by SVA with toluene to form spheres and then
18 re-annealed with a mixture of heptane and toluene to form cylinders.⁶⁵ The two steps took a total
19 of 25 min, and the film had a nanostructure with better order than an equivalent film annealed with
20 only heptane/toluene SVA for the same time period.⁶⁵ This process with multiple annealing steps
21 was further extended to produce non-standard morphologies with immersion annealing. For
22 example, short (< 10 s) exposure to a solvent mixture of heptane/ethanol or heptane/toluene
23 generated core-shell dots and core-shell lines, respectively.⁶⁵ This study suggests that sequential
24 processing of BP nanostructures may be a promising paradigm to efficiently fabricate high-quality
25 morphologies.
26
27

28 Another class of polymers that is challenging to process effectively for nanostructure
29 development is UHMW BPs. These systems produce features >100 nm in size and are attractive
30 for cost-effective functional surfaces and photonics applications.^{86, 87} UHMW BPs present a unique
31 challenge for nanostructure development because of the high kinetic barriers associated with chain
32 mobility, including the presence of entanglements.⁸⁸ Routes to overcome these issues have focused
33 on new additives to provide mobility to the polymer, such as nonvolatile solvents and low
34 molecular weight homopolymers.^{84, 89} Cummins *et al.* demonstrated that use of a low vapor
35 pressure solvent (e.g., propylene glycol methyl ether acetate) to cast a film can reduce the
36 necessary SVA time from ~24 h to ~1 h.⁸⁴ Similarly, low molecular weight homopolymers have
37 been shown to plasticize BPs for improved ordering kinetics during SVA (**Figure 5d**).⁶⁶ With
38 subsequent thermal annealing, the plasticizing homopolymers can segregate into their respective
39 compatible blocks leading to the production of high-quality nanostructures.⁶⁶
40
41

42 A requirement for many lower-cost, large-area nanotechnology applications is continuous
43 manufacturing, often with R2R processing.¹⁴ Batch operations generally are more expensive and
44 have lower throughput, and many of the best-established BP thin-film methods to date operate in
45 this mode. For example, batch techniques for film casting such as drop casting and spin coating
46 are used frequently in a lab setting, but there are alternatives, *e.g.*, slot-die coating, dip coating,
47 and flow coating that are available for R2R production.^{15, 16} Continuous annealing routes, on the
48 other hand, have been a challenge to develop. RSVA and CZA, discussed previously, are exciting
49 advances in part because they can anneal BP nanostructures in a manner that is R2R compatible.
50 Another approach is direct immersion annealing (DIA), in which a film is submerged in a carefully
51 chosen mixture of good and poor solvents (**Figure 6a**).⁷³ DIA is notable because it anneals BPs
52 via solvent swelling without the use of vapor as the means of delivery. Furthermore, the time to
53
54
55
56

equilibrate and quench the swollen films is faster for DIA than for conventional SVA.⁷³ Karim and coworkers demonstrated that DIA with a properly tuned solvent mixture can develop poly(styrene-*b*-methyl methacrylate) as well as poly(styrene-*b*-2-vinylpyridine) nanostructures, but formation of large-grain patterns still required immersion annealing times on the order of hours.⁷³ Further efforts focused on DIA also have demonstrated that the method can be extended to nanolithographically patterned high- χ BPs,⁹⁰ as well as BPs highly-filled with nanoparticles.⁹¹

As opposed to reintroducing solvent into a thin film, it also is possible to cast BPs from a mixture of volatile and nonvolatile solvents to slow the evaporation so the thin-film nanostructure can develop (**Figure 6b** and **6c**).^{74, 92} Three notable variations on this theme have produced well-ordered BP thin films: nonvolatile solvent vapor annealing,⁹² plasticizer assisted solvent annealing, and solvent evaporation annealing.⁷⁴ In contrast to fast evaporation from typical solvents used for film casting (e.g., toluene, ~1,000 nm/s), the drying rates for the nonvolatile solvents vary from <0.1 nm/s to ~4 nm/s.⁷⁴ The relatively long drying times for these nonvolatile solvents enable BPs to develop their nanostructure without the need for an enclosure. Furthermore, these methods easily integrate into R2R processing, as they simply require adjusting the casting solution and providing ample time for the nanostructures to develop.

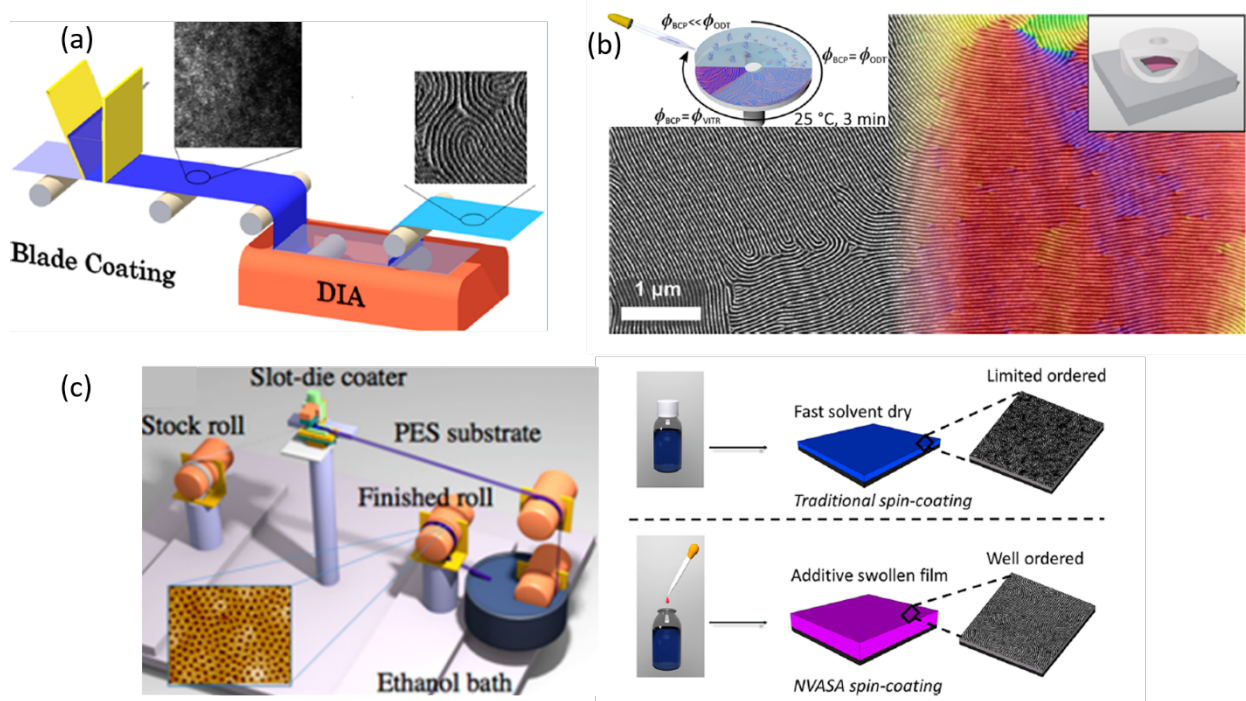


Figure 6. R2R compatible annealing methods. (a) Illustration of DIA. After a film is coated, it is submerged in a mixture of good and bad solvents (e.g., acetone and heptane, respectively, for poly(styrene-*b*-methyl methacrylate)) to anneal the BP without the use of solvent vapors. Reproduced from ref. 73. Copyright 2015 American Chemical Society. (b) Schematic representation of BP casting from a mixture of nonvolatile and volatile solvents. Scanning electron microscopy image of the resulting BP morphology with a false-color orientation map. Reproduced from ref. 61. Copyright 2020 American Chemical Society. (c) Nonvolatile solvent vapor annealing in a R2R printing process. After coating and annealing, the nonvolatile solvent is removed by submerging in an ethanol bath. The addition of a nonvolatile solvent to the casting solution results

in a swollen state for the thin film after casting until the residual solvent is removed. Reproduced from ref. 92. Copyright 2019 American Chemical Society.

Despite the progress of new techniques to anneal BP thin-film nanostructures faster and with better compatibility for continuous fabrication, there are still several key limitations. In particular, effective production of large grain structures or long-range order continues to be a challenge — this drawback may be due the undirected nature of most annealing methods.⁶⁷ Without an external driving force to bias the orientation of the thin film's nanostructure, aligned patterns are difficult to produce.¹⁷

3.2 Shear-Based Directed Self-Assembly

DSA methods have attracted significant attention for their ability to generate nanopatterns that have long-range order or assemblies with larger grain structures.²¹ Although many DSA techniques have been investigated, these technologies have not significantly transitioned into industrial processes. Shear alignment approaches have been demonstrated with various polymer systems, and the modes of operation have expanded over time to function with different means of applying shear and plasticization.^{52, 54, 55, 63, 93} One form of shear alignment involves lateral displacement of the elastomer while the system is heated to temperatures above the T_g s of the polymer blocks.⁵⁴⁻⁵⁶ Another version uses solvent vapor, and instead of lateral displacement, the shear is produced by the solvent drying front contracting the elastomeric pad.^{51, 52, 57} Although both approaches generate well-aligned patterns, they are slow and restricted to operation in batch-mode. As with the discussion on annealing, the development of fast and continuous processing operations is critical to industrial adoption (**Table 2**).

Table 2. Key characteristics of various shear-based DSA methods

Method	Advantages	Disadvantages	References
Thermal annealing with hard shear	Capable of producing highly aligned nanostructures with low defect-densities	Slow (hours), nonideal for thermally sensitive polymers, limited to batch-mode operation	⁵⁴
Solvent vapor annealing with soft shear (SVA-SS)	Capable of producing highly aligned nanostructures with low defect-densities, compatible with most polymers	Slow (hours), limited to batch mode operation	⁵²
Raster solvent vapor annealing with soft shear (RSVA-SS)	Spatially controllable, compatible with most polymers, capable of being adapted for continuous operation	Slow linear speeds (10 $\mu\text{m/s}$), limited with respect to sharpness of the transition between annealed and unannealed regions	²²
Cold zone annealing with soft shear (CZA-SS)	Fast linear speeds (200 $\mu\text{m/s}$), capable of being adapted for continuous operation	Nonideal for thermally sensitive polymers	⁶²
Soft shear laser zone annealing (SS-LZA)	Fast linear speeds (320 $\mu\text{m/s}$)	Limited to batch-mode operation due to vacuum, nonideal for thermally sensitive polymers,	⁶¹

		restricted to light absorbing substrates	
--	--	--	--

The Epps group has demonstrated RSVA with soft shear (RSVA-SS) by placing a PDMS pad on top of a thin film and performing RSVA. The elastomer swelled and deswelled to orient BP nanopatterns on the basis of rastering direction (**Figure 7a**).²² A unique benefit of this technique was that it enabled spatial control over the direction of nanostructure alignment. This method also can be adapted to other modes of solvent delivery. As opposed to using a needle-like nozzle to focus solvent vapor flow, a flat nozzle with a wide slit was employed to shear align over wider areas for more effective continuous processing.²² The primary drawback with this approach is that it has not yet been optimized for faster alignment — although high quality structures were produced at 10 $\mu\text{m}/\text{s}$, speeds $>100\mu\text{m}/\text{s}$ had no impact on morphology.²²

Two techniques have been developed that use elastomeric pads with processing speeds on the order of $\sim 100\mu\text{m}/\text{s}$: cold zone annealing with soft shear (CZA-SS) and soft shear laser zone annealing (SS-LZA).^{61, 62, 94} For both methods, a PDMS pad was placed on top of the film, and the nanostructure was aligned by the expansion and contraction of the elastomer. The rapid heating and cooling drive thermal expansion and contraction of the elastomer for thermal zone shear methods; CZA-SS uses a hot wire sandwiched between cold blocks, and SS-LZA uses a focused laser (**Figures 7b and 7c**).^{61, 62} Karim and coworkers demonstrated that CZA-SS could operate at speeds as fast as 200 $\mu\text{m}/\text{s}$ and was compatible with flexible substrates such as polyimide films, a necessary feature for true R2R compatibility.⁹⁴ The key limitation of CZA-SS is that for polymer systems to be aligned effectively, the BP must have a $T_g \ll T_{\text{ODT}}$. SS-LZA has similar constraints with respect to the choice of BPs, and although SS-LZA can operate with speeds near 300 $\mu\text{m}/\text{s}$, this method requires vacuum,⁶¹ and multiple sweeps of the laser were required at the higher speeds. Another important consideration is that all the methods discussed were only shown with a PDMS pad that was placed onto the film surface, which is noteworthy because such an arrangement is suboptimal for R2R processing. Karim and coworkers did propose the use of a PDMS roller as a more compatible option,⁶² but to our knowledge, it has yet to be demonstrated in literature.

A key component of these DSA approaches is that they promote self-assembly to occur with an anisotropic bias. Typically, this process of aligning polymer chains happens concurrently with annealing to form well-ordered structures with few defects. An alternative route to achieve low-defect, long-range films is to apply shear stress briefly to instill ‘latent alignment’ onto the film, and then anneal the sample further to form an aligned, low-defect patterns.⁹⁵ This concept, explored by Majewski and Yager, establishes long-range orientational correlation before phase separation is completed — SS-LZA was used to align poly(styrene-*b*-methyl methacrylate) for a short period (total exposure of 70 ms with sweep speeds of 1280 $\mu\text{m}/\text{s}$), followed by LZA to anneal the film.⁹⁵ Weakly aligned patterns were obtained after the short SS-LZA exposure, and subsequent LZA or oven annealing developed led to highly ordered nanostructures.⁹⁵ This pathway for reorganization also is consistent with the mechanism of SVA-SS discussed in section 2.3 because Shelton *et al.* found that shear alignment involved chain mixing and nanostructure disordering, followed by the formation of small grains with reduced entropic penalties for alignment.²⁷ Further investigation into latent alignment, and the development of new methods that leverage this concept, could lead to significant improvements in BP thin-film processing.

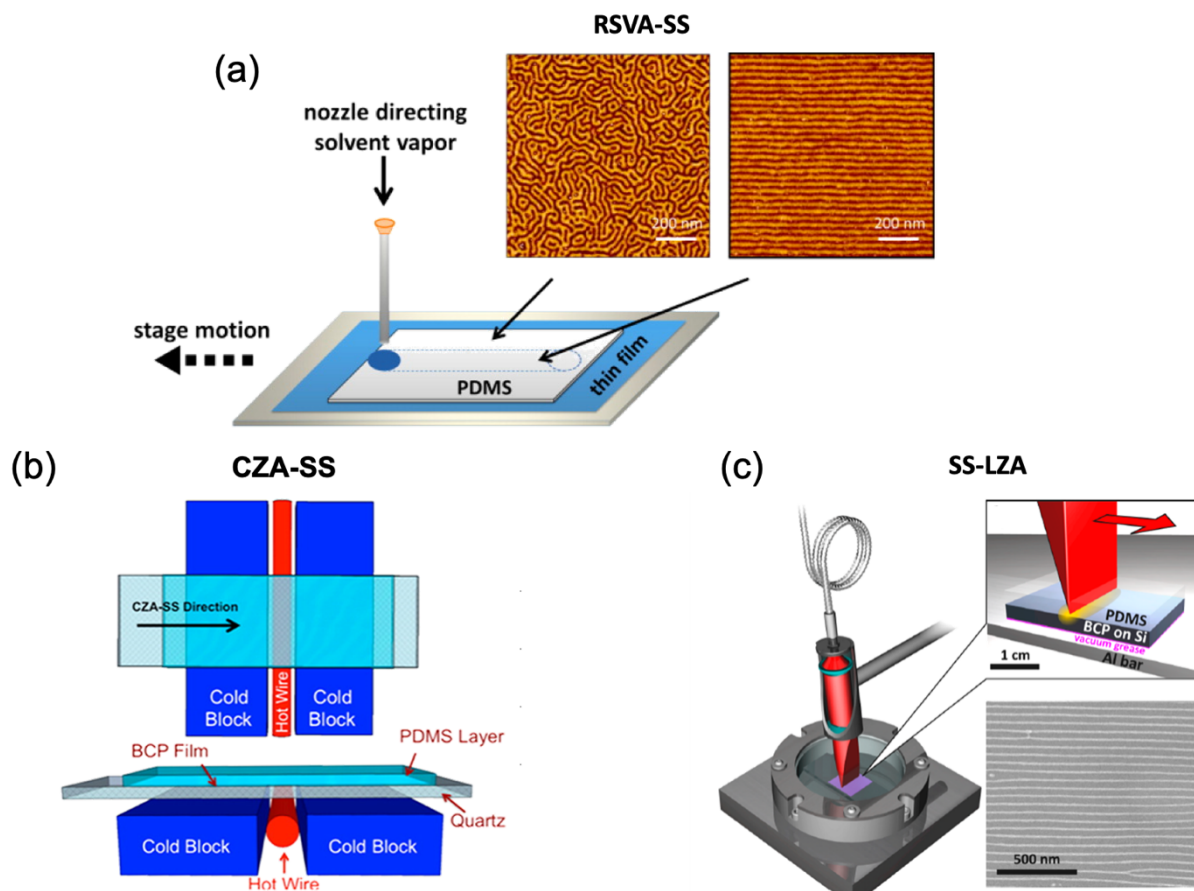


Figure 7. A comparison of different shear-based alignment methods. (a) RSVA-SS, although slower than the other techniques, has the broadest compatibility with BP systems because it uses solvent vapor as opposed to heat. Reproduced from ref. 22. Copyright 2015 American Chemical Society. (b) CZA-SS operates at moderately fast speeds and has been demonstrated with flexible substrates, but it is limited to polymer systems with $T_g \ll T_{ODT}$. Reproduced from ref. 62. Copyright 2012 American Chemical Society. (c) SS-LZA is the fastest approach demonstrated to date, but it has the same polymer constraints as CZA-SS, and the method may not be R2R compatible because the film must be placed in a vacuum chamber. Reproduced from ref. 61. Copyright 2020 American Chemical Society.

4. Conclusion and Outlook

Block polymers have the potential to enable next-generation functional nanomaterials because they can be used for cost-effective production of submicron structures. Specifically, the ability to control the shape and size of features on the basis of composition and molecular weight provides a simple route to pattern large areas in comparison to existing methods. However, the spontaneous nature of microphase separation has the propensity to develop isotropic nanostructures with defects. Without techniques to improve the quality of the assembled features, block polymer thin films cannot be used for many applications. A wide range of methods have been established to control different facets of block polymer thin-film morphologies, but

development is still needed for processes to be compatible with manufacturing infrastructure (e.g., roll-to-roll systems) and produce patterns of consistent quality.

This Spotlight has presented investigations into key aspects of block polymer thin-film nanostructure formation that contribute to the design of effective nanopattern fabrication techniques. The contributions of the Epps group include assessments of processing conditions and analyses of self-assembly pathways. These studies were enabled by combinatorial, gradient, and *in situ* experimental strategies to probe nanostructure formation. Routes to promote perpendicular morphologies were revealed, energetic drivers of wetting behavior were identified, and the effects of these interfacial interactions through the thicknesses of films were determined. Additionally, underlying mechanisms of the development of kinetically trapped states and the promotion of chain mixing *via* shear force were elucidated. These findings provide important insights into self-assembly processes and enable the creation of innovative new methods to direct nanostructure formation quickly and reliably.

Continued efforts are still required to reduce defect densities, improve long-range order, and increase processing speed, especially in roll-to-roll-compatible systems. Significant progress has been made with new techniques to anneal and direct self-assembly of block polymers; for example, the Epps group pioneered raster solvent vapor annealing⁶⁹ and raster solvent vapor annealing with soft shear,²² which are amenable to continuous operation and have faster ordering kinetics than traditional solvent vapor annealing. However, ordering kinetics are slow for most methods, and many other approaches are not compatible with continuous operation. There are two key concepts that could be leveraged to create better techniques to control block polymer nanostructure: latent alignment and sequential processing. Latent alignment uses rapid shear to produce seemingly disordered films with directionality imbued in the polymer chains, and subsequent annealing yields highly oriented patterns.⁹⁵ Sequential routes involve morphological transitions, such as self-assembly into a spherical nanostructure, followed by solvent annealing to make well-ordered cylinders.⁶⁵ Both approaches use ordering pathways to generate low defect-density patterns with faster kinetics than available through a single step process. The extension of these concepts to more directed self-assembly and annealing methods could lead to effective procedures for the rapid fabrication of low defect-density films and help overcome the limitations that hinder adoption of block polymer-based technologies as discussed in the introduction for electronics and membrane applications. For example, a procedure with latent alignment to form well-ordered parallel cylinders followed by annealing to transition the structure to a perpendicular orientation could be an effective way to circumvent the defect-density and throughput issues described in the introduction for BPs to be employed as templates for bit-patterned media and membranes.⁹⁶

An important consideration is to define key performance criteria for specific applications and/or fabrication systems. For example, one of the fastest roll-to-roll compatible method developed to date, cold zone annealing with soft shear, operates at 200 $\mu\text{m/s}$, but desired rates for some relevant industrial roll-to-roll processes can be on the order of 10 cm/s. Additionally, equipment can operate as fast as 15 m/s, and nanofabrication techniques that can reach this speed could be transformative.^{15, 97} Furthermore, new and existing approaches need to be demonstrated with application-relevant systems; the effectiveness of these methods cannot be assumed for all polymers, especially because macromolecular characteristics of the systems (e.g., ultrahigh molecular weight or large Flory-Huggins interaction parameters) can impact critical considerations like ordering kinetics. For instance, the Epps group demonstrated that solvent vapor annealing with soft shear could be used to produce long-range order for star block polymers with large Flory-

Huggins interaction parameters, but achieving the desired nanostructure required carefully chosen solvent mixtures.⁴¹

Another challenge relates to the large parameter spaces involved in block polymer self-assembly. Methods to form a target morphology are impacted by a number of factors, including block chemistry, substrate choice, film deposition method, and film thickness. As such, effective routes to explore parameter spaces are critical to optimize protocols, and gradient or combinatorial screenings are powerful approaches to tackle this challenge. The Epps group pioneered techniques to produce substrates with gradient surface modifications, films with gradient thicknesses, and BPs with nanostructures annealed by combinations of different solvent vapors, and a number of valuable insights were obtained by using these tools. For example, surface energy parameters that affect surface wetting were identified for block polymer, and these results could be used to predict wetting behavior and hole formation size across substrates.³⁶ Also, the through-film effects of substrate/polymer interactions were found to be a function of the long-range decoupled surface energy components.²³ With the development of innovative approaches to anneal or direct self-assembly, such as direct immersion annealing and nonvolatile solvent vapor annealing, there is an opportunity to create new gradient techniques that probe the associated parameter spaces. Furthermore, these high-throughput screening tools highlight a need for improved characterization — faster microscopy that can operate over larger areas also will enable more efficient workflows to assess parameter spaces more quickly and with superior statistical significance.

Also, there still is a significant need to better understand of the mechanisms and pathways of nanostructure formation, and this information gap can be addressed by *in situ* investigations. The Epps group has made contributions to these efforts with *in situ* neutron scattering and reflectivity approaches to study solvent vapor annealing and solvent vapor annealing with soft shear. Two distinct stages of nanostructure reorganization were identified for solvent removal: (1) when the effective glass transition temperature of the harder block is below room temperature, and (2) when the effective glass transition temperature of the harder block is above room temperature. The former condition allows the system to rearrange to have fewer layers in response to a decrease in thickness, whereas the latter condition forces the domain spacing to change in response to variations in film thickness.²⁴ Also, a chain mixing and nanostructure disordering were found to be key components of the intermediate state for block polymers aligned by solvent vapor annealing with soft shear, and solvent alone was insufficient to induce a similar loss of order.²⁷ These results provided critical insights into self-assembly processes during solvent annealing and shear alignment. With a push for faster methods to develop thin film nanostructures, *in situ* approaches capable of rapid data collection such as scattering with high-flux synchrotron beamlines could be instrumental in the investigation of ordering phenomena at shorter timescales.

Finally, the ability to produce complex patterns (e.g., squares, 90° bends, 3-dimensional structures) reliably without lithography remains an ongoing challenge, and these structures are necessary for electronics fabrication.^{98–100} Nonstandard morphologies can be obtained from block polymer blends,¹⁰¹ star block polymers,⁹⁹ or supramolecular assemblies composed of block polymers¹⁰² with constrained chain locations and/or junctions with respect to the interfaces.⁹⁸ However, the increased complexity of these systems creates more challenges that researchers must address; there are both a larger parameter spaces to probe and smaller stability windows for nonstandard morphologies.⁹⁸ A combination of micro- and nanopatterning could be used with these more complicated systems to direct self-assembly and fabricate complex patterns reproducibly.

Overall, block polymers can enable a new generation of functional materials, but methods are needed to form nanostructured films economically and at industrially-relevant scales. With effective tools for high-throughput investigations and *in situ* routes to probe self-assembly, further understanding of microphase separation can be achieved. These insights then can be leveraged to find better ordering pathways with improved kinetics to generate low defect-density patterns quickly. Furthermore, new techniques that take advantage of these breakthroughs will need to be validated for the many constraints of fabrication in industry, such as the substrate, the polymer, the final nanostructure, and the operating speed. As more manufacturing-compatible methods are discovered and tested, the potential of block polymer thin films can be realized in applied environments.

ACKNOWLEDGMENTS

E.R.G. and T.H.E. thank the National Science Foundation (NSF DMR-1610134) and the National Institute of Standards and Technology (NIST; U.S. Department of Commerce - #70NANB12H302) for financial support during the writing of this manuscript. A.G. and T.H.E. thank the NSF - University of Delaware Materials Research Science and Engineering Center DMR-2011824 for financial support during the writing of this manuscript. The statements in this work are those of the authors and do not necessarily reflect the views of NIST or NSF.

ABBREVIATIONS

AFM, atomic force microscopy; benzyl silane, benzyldimethylchlorosilane; BP, block polymer; CZA, cold zone annealing; CZA-SS, cold zone annealing with soft shear; *d*, interlayer spacing; DIA, direct immersion annealing; DSA, directed self-assembly; HPL, hexagonally perforated lamellae; HZA, hot zone annealing; LZA, laser zone annealing; *n*-butyl silane, *n*-butyldimethylchlorosilane; PDMS, polydimethylsiloxane; PMMA-PnBA, poly(methyl methacrylate-*b*-*n*-butyl acrylate); R2R, roll-to-roll; RSVA, raster solvent vapor annealing; RSVA-SS, raster solvent vapor annealing with soft shear; SANS, small-angle neutron scattering; SIS, poly(styrene-*b*-isoprene-*b*-styrene); SS-LZA, soft shear laser zone annealing; SVA, solvent vapor annealing; SVA-SS, solvent vapor annealing with soft shear; T_g , glass transition temperature; T_{ODT} , order-disorder transition temperature; UHMW, ultrahigh molecular weight; χ ; Flory-Huggins interaction parameter.

AUTHOR CONTRIBUTIONS

The article was written by E.R.G. and A.G., and figures were made by E.R.G. and A.G. The article was edited by E.R.G. and T.H.E.

1
2
3 **References**

4

5 1. Park, M.; Harrison, C.; Chaikin, P. M.; Register, R. A.; Adamson, D. H., Block Copolymer
6 Lithography: Periodic Arrays of $\sim 10^{11}$ Holes in 1 Square Centimeter. *Science* **1997**, 276
7 (5317), 1401-1404.

8 2. Li, M.; Ober, C. K., Block Copolymer Patterns and Templates. *Materials Today* **2006**, 9
9 (9), 30-39.

10 3. Yang, X.; Xiao, S.; Hsu, Y.; Feldbaum, M.; Lee, K.; Kuo, D., Directed Self-Assembly of
11 Block Copolymer for Bit Patterned Media with Areal Density of 1.5 Teradot/Inch² and
12 Beyond. *Journal of Nanomaterials* **2013**, 2013, 615896.

13 4. Gou, P.-F.; Zhu, W.-P.; Shen, Z.-Q., Synthesis, Self-Assembly, and Drug-Loading
14 Capacity of Well-Defined Cyclodextrin-Centered Drug-Conjugated Amphiphilic A₁₄B₇
15 Miktoarm Star Copolymers Based on Poly(ϵ -caprolactone) and Poly(ethylene glycol).
16 *Biomacromolecules* **2010**, 11 (4), 934-943.

17 5. Morris, M. A.; Gartner, T. E.; Epps, T. H., III, Tuning Block Polymer Structure, Properties,
18 and Processability for the Design of Efficient Nanostructured Materials Systems.
19 *Macromolecular Chemistry and Physics* **2017**, 218 (5), 1600513.

20 6. Zhang, Y.; Almodovar-Arbelo, N. E.; Weidman, J. L.; Corti, D. S.; Boudouris, B. W.;
21 Phillip, W. A., Fit-for-Purpose Block Polymer Membranes Molecularly Engineered for
22 Water Treatment. *NPJ Clean Water* **2018**, 1 (1), 2.

23 7. Bates, F. S.; Fredrickson, G. H., Block Copolymers—Designer Soft Materials. *Physics*
24 *Today* **1999**, 52 (2), 32-38.

25 8. Cummins, C.; Lundy, R.; Walsh, J. J.; Ponsinet, V.; Fleury, G.; Morris, M. A., Enabling
26 Future Nanomanufacturing Through Block Copolymer Self-Assembly: A Review. *Nano*
27 *Today* **2020**, 35, 100936.

28 9. Hawker, C. J.; Russell, T. P., Block Copolymer Lithography: Merging “Bottom-Up” with
29 “Top-Down” Processes. *MRS Bulletin* **2005**, 30 (12), 952-966.

30 10. Biswas, A.; Bayer, I. S.; Biris, A. S.; Wang, T.; Dervishi, E.; Faupel, F., Advances in Top-
31 Down and Bottom-Up Surface Nanofabrication: Techniques, Applications & Future
32 Prospects. *Advances in Colloid and Interface Science* **2012**, 170 (1-2), 2-27.

33 11. Rodgers, P., Chip maker turns to self-assembly. *Nature Nanotechnology* **2007**, doi:
34 10.1038/nnano.2007.170.

35 12. Murphy, J. N.; Harris, K. D.; Buriak, J. M., Automated Defect and Correlation Length
36 Analysis of Block Copolymer Thin Film Nanopatterns. *PLOS ONE* **2015**, 10 (7),
37 e0133088.

38 13. Kamon, M. Will Directed Self-Assembly Pattern 14nm DRAM?
39 <https://www.coventor.com/blog/will-directed-self-assembly-pattern-14nm-dram/>
40 (accessed 2021-05-22).

41 14. Singh, G.; Batra, S.; Zhang, R.; Yuan, H.; Yager, K. G.; Cakmak, M.; Berry, B.; Karim,
42 A., Large-Scale Roll-to-Roll Fabrication of Vertically Oriented Block Copolymer Thin
43 Films. *ACS Nano* **2013**, 7 (6), 5291-5299.

44 15. Søndergaard, R.; Hösel, M.; Angmo, D.; Larsen-Olsen, T. T.; Krebs, F. C., Roll-to-Roll
45 Fabrication of Polymer Solar Cells. *Materials Today* **2012**, 15 (1-2), 36-49.

46 16. Shan, X. C.; Mohahidin, M. B.; Lu, A. C. W., Roll-to-roll (R2R) Hot Embossing for
47 Structuring 3D Microstructures on Polymer Films. In *2012 IEEE 14th Electronics*
48 *Packaging Technology Conference (EPTC)*, 2012; pp 568-571.

49

50

51

52

53

54

55

56

57

58

59

60

1
2
3 17. Gunkel, I., Directing Block Copolymer Self-Assembly on Patterned Substrates. *Small*
4 **2018**, *14* (46), 1802872.
5
6 18. Luo, M.; Seppala, J. E.; Albert, J. N. L.; Lewis, R. L.; Mahadevapuram, N.; Stein, G. E.;
7 Epps, T. H., III, Manipulating Nanoscale Morphologies in Cylinder-Forming Poly(styrene-
8 b-isoprene-b-styrene) Thin Films Using Film Thickness and Substrate Surface Chemistry
9 Gradients. *Macromolecules* **2013**, *46* (5), 1803-1811.
10
11 19. Albert, J. N. L.; Baney, M. J.; Stafford, C. M.; Kelly, J. Y.; Epps, T. H., III, Generation of
12 Monolayer Gradients in Surface Energy and Surface Chemistry for Block Copolymer Thin
13 Film Studies. *ACS Nano* **2009**, *3* (12), 3977-3986.
14
15 20. Sinturel, C.; Vayer, M.; Morris, M.; Hillmyer, M. A., Solvent Vapor Annealing of Block
16 Polymer Thin Films. *Macromolecules* **2013**, *46* (14), 5399-5415.
17
18 21. Hu, H.; Gopinadhan, M.; Osuji, C. O., Directed Self-Assembly of Block Copolymers: a
19 Tutorial Review of Strategies for Enabling Nanotechnology with Soft Matter. *Soft Matter*
20 **2014**, *10* (22), 3867-3889.
21
22 22. Luo, M.; Scott, D. M.; Epps, T. H., III, Writing Highly Ordered Macroscopic Patterns in
23 Cylindrical Block Polymer Thin Films via Raster Solvent Vapor Annealing and Soft Shear.
24 *ACS Macro Letters* **2015**, *4* (5), 516-520.
25
26 23. Shelton, C. K.; Epps, T. H., III, Mapping Substrate Surface Field Propagation in Block
27 Polymer Thin Films. *Macromolecules* **2016**, *49* (2), 574-580.
28
29 24. Shelton, C. K.; Jones, R. L.; Dura, J. A.; Epps, T. H., III, Tracking Solvent Distribution in
30 Block Polymer Thin Films during Solvent Vapor Annealing with *in Situ* Neutron
31 Scattering. *Macromolecules* **2016**, *49* (19), 7525-7534.
32
33 25. Zou, Y.; Zhou, X.; Ma, J.; Yang, X.; Deng, Y., Recent advances in amphiphilic block
34 copolymer templated mesoporous metal-based materials: assembly engineering and
35 applications. *Chemical Society Reviews* **2020**, *49* (4), 1173-1208.
36
37 26. Brilmayer, R.; Förster, C.; Zhao, L.; Andrieu-Brunsen, A., Recent trends in nanopore
38 polymer functionalization. *Current Opinion in Biotechnology* **2020**, *63*, 200-209.
39
40 27. Shelton, C. K.; Jones, R. L.; Epps, T. H., III, Kinetics of Domain Alignment in Block
41 Polymer Thin Films during Solvent Vapor Annealing with Soft Shear: An *in Situ* Small-
42 Angle Neutron Scattering Investigation. *Macromolecules* **2017**, *50* (14), 5367-5376.
43
44 28. Bilchak, C. R.; Govind, S.; Contreas, G.; Rasin, B.; Maguire, S. M.; Composto, R. J.;
45 Fakhraai, Z., Kinetic Monitoring of Block Copolymer Self-Assembly Using *in Situ*
46 Spectroscopic Ellipsometry. *ACS Macro Letters* **2020**, *9* (8), 1095-1101.
47
48 29. Mansky, P.; Lui, Y.; Huang, E.; Russell, T. P.; Hawker, C. J., Controlling Polymer-Surface
49 Interactions with Random Copolymer Brushes. *Science* **1997**, *275* (5305), 1458-1460.
50
51 30. Epps, T. H., III; Delongchamp, D. M.; Fasolka, M. J.; Fischer, D. A.; Jablonski, E. L.,
52 Substrate Surface Energy Dependent Morphology and Dewetting in an ABC Triblock
53 Copolymer Film. *Langmuir* **2007**, *23* (6), 3355-3362.
54
55 31. Seshimo, T.; Bates, C. M.; Dean, L. M.; Cushen, J. D.; Durand, W. J.; Maher, M. J.; Ellison,
56 C. J.; Willson, C. G., Block Copolymer Orientation Control Using a Top-Coat Surface
57 Treatment. *Journal of Photopolymer Science and Technology* **2012**, *25* (1), 125-130.
58
59 32. Bates, C. M.; Strahan, J. R.; Santos, L. J.; Mueller, B. K.; Bamgbade, B. O.; Lee, J. A.;
60 Katzenstein, J. M.; Ellison, C. J.; Willson, C. G., Polymeric Cross-Linked Surface
Treatments for Controlling Block Copolymer Orientation in Thin Films. *Langmuir* **2011**,
27 (5), 2000-2006.

1
2
3 33. Winesett, D. A.; Story, S.; Luning, J.; Ade, H., Tuning Substrate Surface Energies for
4 Blends of Polystyrene and Poly(methyl methacrylate). *Langmuir* **2003**, *19* (20), 8526-
5 8535.

6 34. Albert, J. N. L.; Kim, J. D.; Stafford, C. M.; Epps, T. H., III, Controlled Vapor Deposition
7 Approach to Generating Substrate Surface Energy/Chemistry Gradients. *Review of*
8 *Scientific Instruments* **2011**, *82* (6), 065103.

9 35. Julthongpiput, D.; Fasolka, M. J.; Zhang, W.; Nguyen, T.; Amis, E. J., Gradient Chemical
10 Micropatterns: A Reference Substrate for Surface Nanometrology. *Nano Letters* **2005**, *5*
11 (8), 1535-1540.

12 36. Shelton, C. K.; Epps, T. H., III, Decoupling Substrate Surface Interactions in Block
13 Polymer Thin Film Self-Assembly. *Macromolecules* **2015**, *48* (13), 4572-4580.

14 37. Xu, T.; Hawker, C. J.; Russell, T. P., Interfacial Interaction Dependence of Microdomain
15 Orientation in Diblock Copolymer Thin Films. *Macromolecules* **2005**, *38* (7), 2802-2805.

16 38. Vayer, M.; Vital, A.; Sinturel, C., New Insights into Polymer-Solvent Affinity in Thin
17 Films. *European Polymer Journal* **2017**, *93*, 132-139.

18 39. Albert, J. N. L.; Young, W.-S.; Lewis, R. L.; Bogart, T. D.; Smith, J. R.; Epps, T. H., III,
19 Systematic Study on the Effect of Solvent Removal Rate on the Morphology of Solvent
20 Vapor Annealed ABA Triblock Copolymer Thin Films. *ACS Nano* **2012**, *6* (1), 459-466.

21 40. Gotrik, K. W.; Hannon, A. F.; Son, J. G.; Keller, B.; Alexander-Katz, A.; Ross, C. A.,
22 Morphology Control in Block Copolymer Films Using Mixed Solvent Vapors. *ACS Nano*
23 **2012**, *6* (9), 8052-8059.

24 41. Sung, S. H.; Farnham, W. B.; Burch, H. E.; Brun, Y.; Qi, K.; Epps, T. H., III, Directional
25 Self-Assembly of Fluorinated Star Block Polymer Thin Films Using Mixed Solvent Vapor
26 Annealing. *Journal of Polymer Science Part B: Polymer Physics* **2019**, *57* (24), 1663-1672.

27 42. Albert, J. N. L.; Bogart, T. D.; Lewis, R. L.; Beers, K. L.; Fasolka, M. J.; Hutchison, J. B.;
28 Vogt, B. D.; Epps, T. H., III, Gradient Solvent Vapor Annealing of Block Copolymer Thin
29 Films Using a Microfluidic Mixing Device. *Nano Letters* **2011**, *11* (3), 1351-1357.

30 43. Kim, G.; Libera, M., Morphological Development in Solvent-Cast
31 Polystyrene-Polybutadiene-Polystyrene (SBS) Triblock Copolymer Thin Films.
32 *Macromolecules* **1998**, *31* (8), 2569-2577.

33 44. Phillip, W. A.; Hillmyer, M. A.; Cussler, E. L., Cylinder Orientation Mechanism in Block
34 Copolymer Thin Films Upon Solvent Evaporation. *Macromolecules* **2010**, *43* (18), 7763-
35 7770.

36 45. Gunkel, I.; Gu, X.; Sun, Z.; Schaible, E.; Hexemer, A.; Russell, T. P., An *in Situ* GISAXS
37 Study of Selective Solvent Vapor Annealing in Thin Block Copolymer Films: Symmetry
38 Breaking of In-Plane Sphere Order Upon Deswelling. *Journal of Polymer Science Part B:*
39 *Polymer Physics* **2016**, *54* (2), 331-338.

40 46. Modi, A.; Karim, A.; Tsige, M., Solvent and Substrate Induced Synergistic Ordering in
41 Block Copolymer Thin Films. *Macromolecules* **2018**, *51* (18), 7186-7196.

42 47. Raybin, J. G.; Sibener, S. J., *in Situ* Visualization of Solvent Swelling Dynamics in Block
43 Copolymer Films with Atomic Force Microscopy. *Macromolecules* **2019**, *52* (15), 5985-
44 5994.

45 48. Müller-Buschbaum, P., GISAXS and GISANS as Metrology Technique for Understanding
46 the 3D Morphology of Block Copolymer Thin Films. *European Polymer Journal* **2016**, *81*,
47 470-493.

48
49
50
51
52
53
54
55
56
57
58
59
60

1
2
3 49. Smilgies, D. M., GISAXS: A Versatile Tool to Assess Structure and Self-Assembly
4 Kinetics in Block Copolymer Thin Films. *Journal of Polymer Science* **2021**, Article ASAP,
5 doi: 10.1002/pol.20210244.
6 50. Bita, I.; Yang, J. K. W.; Jung, Y. S.; Ross, C. A.; Thomas, E. L.; Berggren, K. K.,
7 Graphoepitaxy of Self-Assembled Block Copolymers on Two-Dimensional Periodic
8 Patterned Templates. *Science* **2008**, 321 (5891), 939-943.
9 51. Zhang, C.; Cavicchi, K. A.; Li, R.; Yager, K. G.; Fukuto, M.; Vogt, B. D., Thickness Limit
10 for Alignment of Block Copolymer Films Using Solvent Vapor Annealing with Shear.
11 *Macromolecules* **2018**, 51 (11), 4213-4219.
12 52. Qiang, Z.; Zhang, Y.; Groff, J. A.; Cavicchi, K. A.; Vogt, B. D., A Generalized Method for
13 Alignment of Block Copolymer Films: Solvent Vapor Annealing with Soft Shear. *Soft
14 Matter* **2014**, 10 (32), 6068-6076.
15 53. Majewski, P. W.; Gopinadhan, M.; Osuji, C. O., Magnetic Field Alignment of Block
16 Copolymers and Polymer Nanocomposites: Scalable Microstructure Control in Functional
17 Soft Materials. *Journal of Polymer Science Part B: Polymer Physics* **2012**, 50 (1), 2-8.
18 54. Angelescu, D. E.; Waller, J. H.; Adamson, D. H.; Deshpande, P.; Chou, S. Y.; Register, R.
19 A.; Chaikin, P. M., Macroscopic Orientation of Block Copolymer Cylinders in Single-
20 Layer Films by Shearing. *Advanced Materials* **2004**, 16 (19), 1736-1740.
21 55. Wu, M. W.; Register, R. A.; Chaikin, P. M., Shear Alignment of Sphere-Morphology Block
22 Copolymer Thin Films with Viscous Fluid Flow. *Physical Review E* **2006**, 74 (4), 040801.
23 56. Marencic, A. P.; Adamson, D. H.; Chaikin, P. M.; Register, R. A., Shear Alignment and
24 Realignment of Sphere-Forming and Cylinder-Forming Block-Copolymer Thin Films.
25 *Physical Review E* **2010**, 81 (1), 011503.
26 57. Qiang, Z.; Zhang, L.; Stein, G. E.; Cavicchi, K. A.; Vogt, B. D., Unidirectional Alignment
27 of Block Copolymer Films Induced by Expansion of a Permeable Elastomer during Solvent
28 Vapor Annealing. *Macromolecules* **2014**, 47 (3), 1109-1116.
29 58. Raybin, J. G.; Murphy, J. G.; Dolejsi, M.; Sibener, S. J., Direct Imaging of Interfacial
30 Fluctuations in Confined Block Copolymer with in Situ Slow-Scan-Disabled Atomic Force
31 Microscopy. *ACS Nano* **2019**, 13 (10), 11741-11752.
32 59. Maret, M.; Tiron, R.; Chevalier, X.; Gergaud, P.; Gharbi, A.; Lapeyre, C.; Pradelles, J.;
33 Jousseaume, V.; Fleury, G.; Hadzioannou, G.; Boudet, N.; Navarro, C., Probing Self-
34 Assembly of Cylindrical Morphology Block Copolymer Using in Situ and ex Situ Grazing
35 Incidence Small-Angle X-ray Scattering: The Attractive Case of Graphoepitaxy.
36 *Macromolecules* **2014**, 47 (20), 7221-7229.
37 60. Gopinadhan, M.; Majewski, P. W.; Choo, Y.; Osuji, C. O., Order-Disorder Transition and
38 Alignment Dynamics of a Block Copolymer Under High Magnetic Fields by *in Situ* X-Ray
39 Scattering. *Physical Review Letters* **2013**, 110 (7), 078301.
40 61. Leniart, A. A.; Pula, P.; Sitkiewicz, A.; Majewski, P. W., Macroscopic Alignment of Block
41 Copolymers on Silicon Substrates by Laser Annealing. *ACS Nano* **2020**, 14 (4), 4805-4815.
42 62. Singh, G.; Yager, K. G.; Berry, B.; Kim, H.-C.; Karim, A., Dynamic Thermal Field-
43 Induced Gradient Soft-Shear for Highly Oriented Block Copolymer Thin Films. *ACS Nano*
44 **2012**, 6 (11), 10335-10342.
45 63. Davis, R. L.; Michal, B. T.; Chaikin, P. M.; Register, R. A., Progression of Alignment in
46 Thin Films of Cylinder-Forming Block Copolymers upon Shearing. *Macromolecules* **2015**,
47 48 (15), 5339-5347.
48
49
50
51
52
53
54
55
56
57
58
59
60

1
2
3 64. Fasolka, M. J.; Mayes, A. M., Block Copolymer Thin Films: Physics and Applications. *Annual Review of Materials Research* **2001**, *31* (1), 323-355.
4
5 65. Choi, Y. J.; Byun, M. H.; Park, T. W.; Choi, S.; Bang, J.; Jung, H.; Cho, J.-H.; Kwon, S.-
6 H.; Kim, K. H.; Park, W. I., Rapid and Cyclable Morphology Transition of High- χ Block
7 Copolymers via Solvent Vapor-Immersion Annealing for Nanoscale Lithography. *ACS
8 Applied Nano Materials* **2019**, *2* (3), 1294-1301.
9
10 66. Doerk, G. S.; Li, R.; Fukuto, M.; Yager, K. G., Wet Brush Homopolymers as “Smart
11 Solvents” for Rapid, Large Period Block Copolymer Thin Film Self-Assembly. *Macromolecules* **2020**, *53* (3), 1098-1113.
12
13 67. Luo, M.; Epps, T. H., III, Directed Block Copolymer Thin Film Self-Assembly: Emerging
14 Trends in Nanopattern Fabrication. *Macromolecules* **2013**, *46* (19), 7567-7579.
15
16 68. Hashimoto, T.; Bodycomb, J.; Funaki, Y.; Kimishima, K., The Effect of Temperature
17 Gradient on the Microdomain Orientation of Diblock Copolymers Undergoing an
18 Order-Disorder Transition. *Macromolecules* **1999**, *32* (3), 952-954.
19
20 69. Seppala, J. E.; Lewis, R. L.; Epps, T. H., III, Spatial and Orientation Control of Cylindrical
21 Nanostructures in ABA Triblock Copolymer Thin Films by Raster Solvent Vapor
22 Annealing. *ACS Nano* **2012**, *6* (11), 9855-9862.
23
24 70. Berry, B. C.; Bosse, A. W.; Douglas, J. F.; Jones, R. L.; Karim, A., Orientational Order in
25 Block Copolymer Films Zone Annealed below the Order-Disorder Transition
26 Temperature. *Nano Letters* **2007**, *7* (9), 2789-2794.
27
28 71. Bodycomb, J.; Funaki, Y.; Kimishima, K.; Hashimoto, T., Single-Grain Lamellar
29 Microdomain from a Diblock Copolymer. *Macromolecules* **1999**, *32* (6), 2075-2077.
30
31 72. Majewski, P. W.; Yager, K. G., Millisecond Ordering of Block Copolymer Films via
32 Photothermal Gradients. *ACS Nano* **2015**, *9* (4), 3896-3906.
33
34 73. Modi, A.; Bhaway, S. M.; Vogt, B. D.; Douglas, J. F.; Al-Enizi, A.; Elzatahry, A.; Sharma,
35 A.; Karim, A., Direct Immersion Annealing of Thin Block Copolymer Films. *ACS Applied
36 Materials & Interfaces* **2015**, *7* (39), 21639-21645.
37
38 74. Leniart, A. A.; Pula, P.; Tsai, E. H. R.; Majewski, P. W., Large-Grained Cylindrical Block
39 Copolymer Morphologies by One-Step Room-Temperature Casting. *Macromolecules*
40 **2020**, *53* (24), 11178-11189.
41
42 75. Mita, K.; Tanaka, H.; Saijo, K.; Takenaka, M.; Hashimoto, T., Macroscopically Oriented
43 Lamellar Microdomains Created by “Cold Zone-Heating” Method Involving OOT.
44 *Polymer* **2008**, *49* (23), 5146-5157.
45
46 76. Yager, K. G.; Fredin, N. J.; Zhang, X.; Berry, B. C.; Karim, A.; Jones, R. L., Evolution of
47 Block-Copolymer Order Through a Moving Thermal Zone. *Soft Matter* **2010**, *6* (1), 92-99.
48
49 77. Majewski, P. W.; Yager, K. G., Rapid Ordering of Block Copolymer Thin Films. *J. Phys.:
50 Condens. Matter* **2016**, *28* (40), 403002.
51
52 78. Samant, S.; Hailu, S. T.; Al-Enizi, A. M.; Karim, A.; Raghavan, D., Orientation Control in
53 Nanoparticle Filled Block Copolymer Cold Zone Annealed Films. *Journal of Polymer
54 Science Part B: Polymer Physics* **2015**, *53* (8), 604-614.
55
56 79. Singer, J. P.; Gotrik, K. W.; Lee, J.-H.; Kooi, S. E.; Ross, C. A.; Thomas, E. L., Alignment
57 and Reordering of a Block Copolymer by Solvent-Enhanced Thermal Laser Direct Write.
58 *Polymer* **2014**, *55* (7), 1875-1882.
59
60 80. Jin, H. M.; Lee, S. H.; Kim, J. Y.; Son, S.-W.; Kim, B. H.; Lee, H. K.; Mun, J. H.; Cha, S.
K.; Kim, J. S.; Nealey, P. F.; Lee, K. J.; Kim, S. O., Laser Writing Block Copolymer Self-
Assembly on Graphene Light-Absorbing Layer. *ACS Nano* **2016**, *10* (3), 3435-3442.

1
2
3 81. Gotrik, K. W.; Ross, C. A., Solvothermal Annealing of Block Copolymer Thin Films. *Nano Letters* **2013**, *13* (11), 5117-5122.

4 82. Kim, J. M.; Kim, Y.; Park, W. I.; Hur, Y. H.; Jeong, J. W.; Sim, D. M.; Baek, K. M.; Lee, J. H.; Kim, M.-J.; Jung, Y. S., Eliminating the Trade-Off between the Throughput and Pattern Quality of Sub-15 nm Directed Self-Assembly via Warm Solvent Annealing. *Advanced Functional Materials* **2015**, *25* (2), 306-315.

5 83. Sinturel, C.; Bates, F. S.; Hillmyer, M. A., High χ -Low N Block Polymers: How Far Can We Go? *ACS Macro Letters* **2015**, *4* (9), 1044-1050.

6 84. Cummins, C.; Alvarez-Fernandez, A.; Bentaleb, A.; Hadzioannou, G.; Ponsinet, V.; Fleury, G., Strategy for Enhancing Ultrahigh-Molecular-Weight Block Copolymer Chain Mobility to Access Large Period Sizes (>100 nm). *Langmuir* **2020**, *36* (46), 13872-13880.

7 85. Cong, Y.; Zhai, W.; Wu, C., Morphology Evolution of Block Copolymer Blend Thin Films Induced by Solvent Vapor Annealing. *Soft Materials* **2021**, *19* (1), 117-128.

8 86. Yu, N.; Capasso, F., Flat Optics with Designer Metasurfaces. *Nature Materials* **2014**, *13* (2), 139-150.

9 87. Kim, J. Y.; Kim, H.; Kim, B. H.; Chang, T.; Lim, J.; Jin, H. M.; Mun, J. H.; Choi, Y. J.; Chung, K.; Shin, J.; Fan, S.; Kim, S. O., Highly Tunable Refractive Index Visible-Light Metasurface from Block Copolymer Self-Assembly. *Nature Communications* **2016**, *7* (1), 12911.

10 88. Kim, E.; Ahn, H.; Park, S.; Lee, H.; Lee, M.; Lee, S.; Kim, T.; Kwak, E.-A.; Lee, J. H.; Lei, X.; Huh, J.; Bang, J.; Lee, B.; Ryu, D. Y., Directed Assembly of High Molecular Weight Block Copolymers: Highly Ordered Line Patterns of Perpendicularly Oriented Lamellae with Large Periods. *ACS Nano* **2013**, *7* (3), 1952-1960.

11 89. Semenov, A. N., Phase Equilibria in Block Copolymer-Homopolymer Mixtures. *Macromolecules* **2002**, *26* (9), 2273-2281.

12 90. Park, W. I.; Kim, J. M.; Jeong, J. W.; Jung, Y. S., Deep-Nanoscale Pattern Engineering by Immersion-Induced Self-Assembly. *ACS Nano* **2014**, *8* (10), 10009-10018.

13 91. Longanecker, M.; Modi, A.; Dobrynin, A.; Kim, S.; Yuan, G.; Jones, R.; Satija, S.; Bang, J.; Karim, A., Reduced Domain Size and Interfacial Width in Fast Ordering Nanofilled Block Copolymer Films by Direct Immersion Annealing. *Macromolecules* **2016**, *49* (22), 8563-8571.

14 92. Weller, D. W.; Galuska, L.; Wang, W.; Ehlenburg, D.; Hong, K.; Gu, X., Roll-to-Roll Scalable Production of Ordered Microdomains Through Nonvolatile Additive Solvent Annealing of Block Copolymers. *Macromolecules* **2019**, *52* (13), 5026-5032.

15 93. Oh, J.; Shin, M.; Kim, I. S.; Suh, H. S.; Kim, Y.; Kim, J. K.; Bang, J.; Yeom, B.; Son, J. G., Shear-Rolling Process for Unidirectionally and Perpendicularly Oriented Sub-10-nm Block Copolymer Patterns on the 4 in Scale. *ACS Nano* **2021**, *15* (5), 8549-8558.

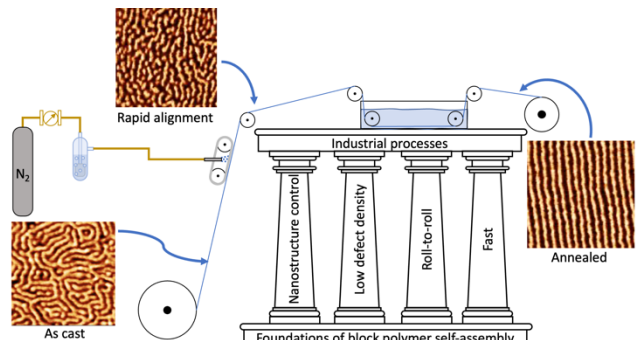
16 94. Samant, S. P.; Grabowski, C. A.; Kisslinger, K.; Yager, K. G.; Yuan, G.; Satija, S. K.; Durstock, M. F.; Raghavan, D.; Karim, A., Directed Self-Assembly of Block Copolymers for High Breakdown Strength Polymer Film Capacitors. *ACS Applied Materials & Interfaces* **2016**, *8* (12), 7966-7976.

17 95. Majewski, P. W.; Yager, K. G., Latent Alignment in Pathway-Dependent Ordering of Block Copolymer Thin Films. *Nano Letters* **2015**, *15* (8), 5221-5228.

18 96. Nowak, S. R.; Lachmayr, K. K.; Yager, K. G.; Sita, L. R., Stable Thermotropic 3D and 2D Double Gyroid Nanostructures with Sub-2-nm Feature Size from Scalable Sugar-Polyolefin Conjugates. *Angew Chem Int Ed Engl* **2021**, *60* (16), 8710-8716.

19
20
21
22
23
24
25
26
27
28
29
30
31
32
33
34
35
36
37
38
39
40
41
42
43
44
45
46
47
48
49
50
51
52
53
54
55
56
57
58
59
60

1
2
3 97. Morse, J. D. *Nanofabrication Technologies for Roll-to-Roll Processing*; 2011.
4 98. Matsushita, Y.; Takano, A.; Vayer, M.; Sinturel, C., Nonclassical Block Copolymer Self-
5 Assemblies Resulting from a Constrained Location of Chains and Junctions. *Advanced
6 Materials Interfaces* **2020**, 7 (5), 1902007.
7 99. Antoine, S.; Aissou, K.; Mumtaz, M.; Pécastaings, G.; Buffeteau, T.; Fleury, G.;
8 Hadzioannou, G., Nanoscale Archimedean Tilings Formed by 3-Miktoarm Star
9 Terpolymer Thin Films. *Macromolecular Rapid Communications* **2019**, 40 (7), 1800860.
10 100. Javey, A.; Nam; Friedman, R. S.; Yan, H.; Lieber, C. M., Layer-by-Layer Assembly of
11 Nanowires for Three-Dimensional, Multifunctional Electronics. *Nano Letters* **2007**, 7 (3),
12 773-777.
13 101. Guliyeva, A.; Vayer, M.; Warmont, F.; Takano, A.; Matsushita, Y.; Sinturel, C., Transition
14 Pathway between Gyroid and Cylindrical Morphology in Linear Triblock Terpolymer Thin
15 Films. *Macromolecules* **2019**, 52 (17), 6641-6648.
16 102. Lefèvre, N.; Daoulas, K. C.; Müller, M.; Gohy, J.-F. o.; Fustin, C.-A., Self-Assembly in
17 Thin Films of Mixtures of Block Copolymers and Homopolymers Interacting by Hydrogen
18 Bonds. *Macromolecules* **2010**, 43 (18), 7734-7743.
19
20
21
22
23

24 TOC Figure
25

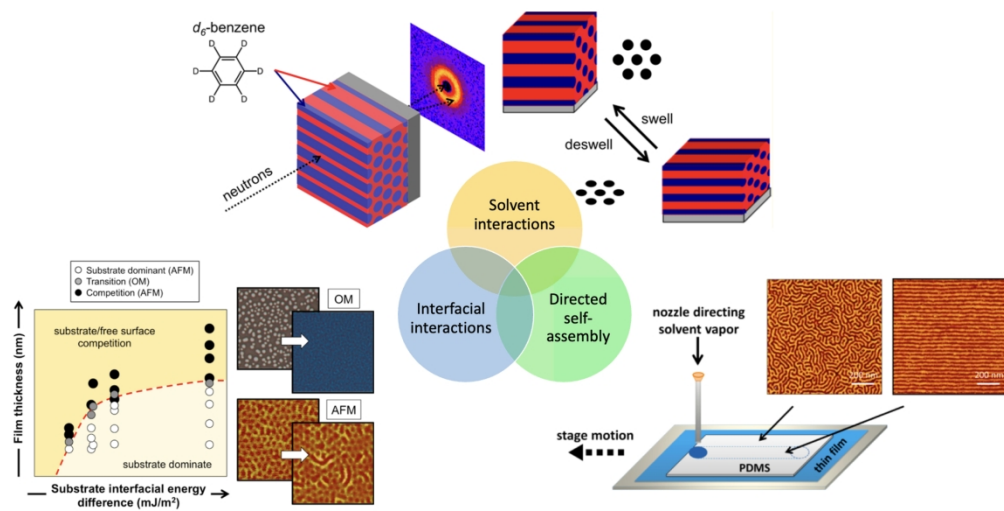


Figure 1. Key aspects of self-assembly and nanostructure control in BP thin films. (Bottom left) The competition between substrate and free surface interfacial interactions is related to film thickness, and the interplay between these factors can impact the surface morphology. Reproduced from ref. 23. Copyright 2016 American Chemical Society. (Top) BPs can reorganize while in a solvent-swollen state; the specific response (e.g., change of number of layers or domain spacing) can vary on the basis of solvent vapor partial pressure and the resulting domain plasticization. Reproduced from ref. 24. Copyright 2016 American Chemical Society. (Bottom right) The application of a shear stress to a BP film can be achieved by solvent vapor to expand and contract an elastomer pad. The solvent vapor also swells the film to provide chain mobility, which can facilitate BP alignment. Reproduced from ref. 22. Copyright 2015 American Chemical Society.

440x221mm (144 x 144 DPI)

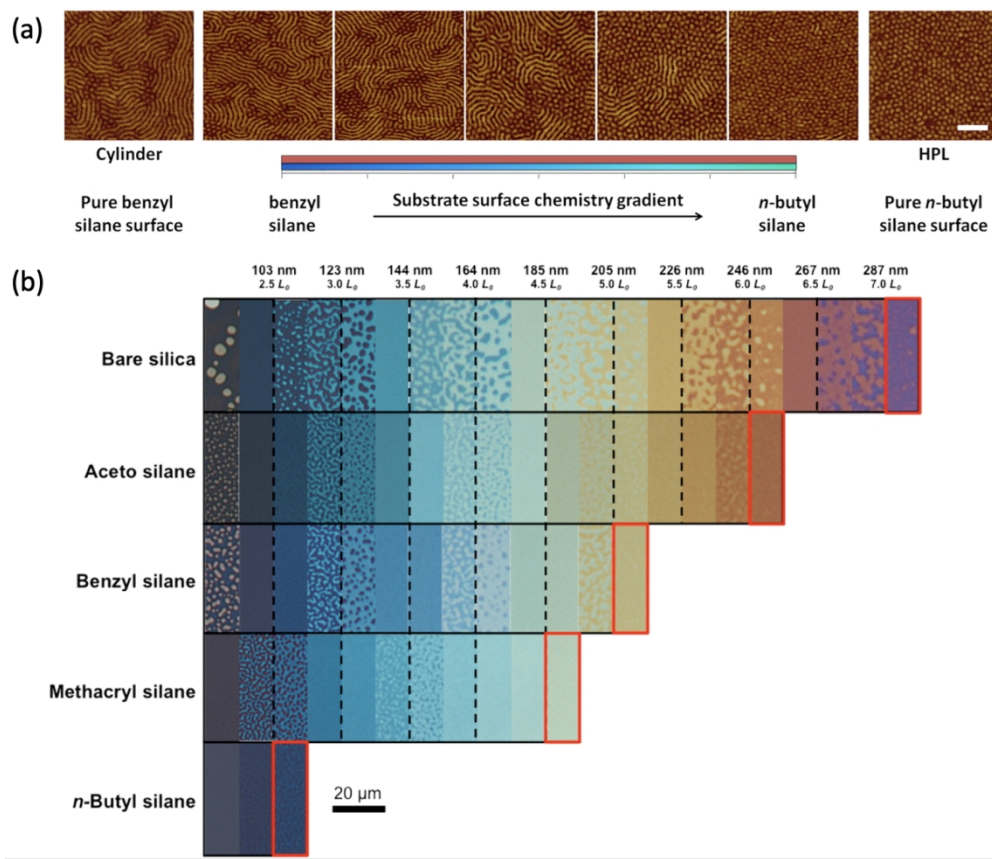


Figure 2. Polymer/substrate interactions. (a) Atomic force microscopy (AFM) phase images of a thermally annealed SIS film cast onto a gradient monolayer. Parallel cylinders were found near the benzyl silane end with a transition to HPL as the n -butyl silane composition on the substrate increased. The scale bar represents 200 nm and applies to all images. Reproduced from ref. 18. Copyright 2013 American Chemical Society. (b) Composite optical microscopy images of gradient thickness PMMA-PnBA films on various substrates. Island/hole structures were formed at integer or half integer domain spacings for asymmetric (bare silica, aceto silane, benzyl silane) and symmetric (methacryl silane, n -butyl silane) wetting substrates, respectively. The red boxes correspond to critical film thicknesses at which island/hole formations were expected but not present, which indicates a transition from a substrate dominant to a substrate/free surface competition regime. The scale bar applies to all micrographs. Reproduced from ref. 23. Copyright 2016 American Chemical Society.

293x250mm (144 x 144 DPI)

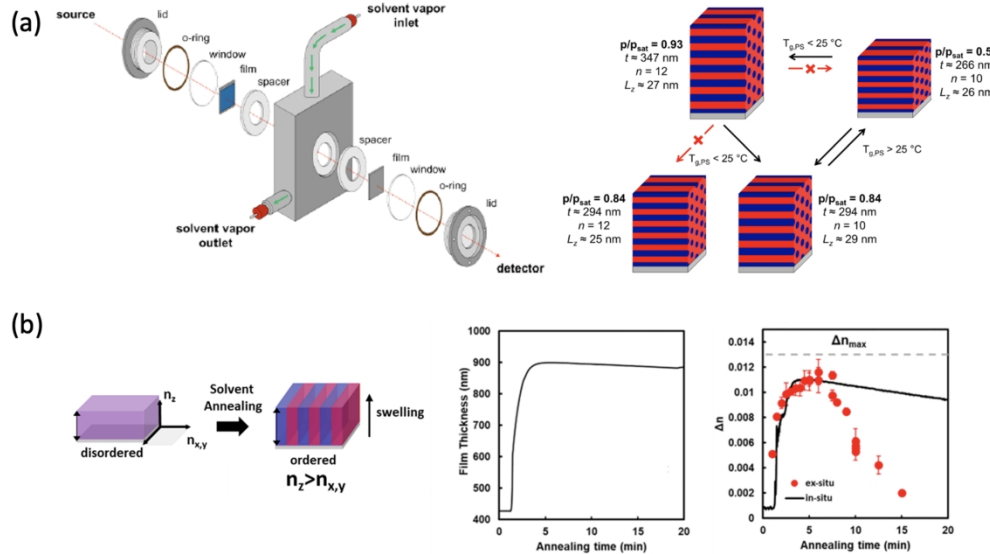


Figure 3. *In situ* studies by SANS and spectroscopic ellipsometry on BP thin films. (a) Schematic of a sample cell for *in situ* SANS measurements with SVA, and an illustration of the different morphological change the polymer layers went through during swelling and deswelling on the basis of the environmental conditions. Reproduced from ref. 24. Copyright 2016 American Chemical Society. (b) Kinetic monitoring of poly(styrene-*b*-2-vinylpyridine) thin-film self-assembly by *in situ* spectroscopic ellipsometry with chloroform vapor at a steady vapor pressure. Film thickness (left), *in situ* birefringence ($\Delta n = n_z - n_{x,y}$) (right, black line), and $\langle I \rangle$ *ex situ* birefringence (red circles) data as a function of annealing time. Although birefringence correlated with film thickness initially, *ex situ* birefringence measurements deviated with longer annealing times. Reproduced from ref. 28. Copyright 2020 American Chemical Society.

444x248mm (144 x 144 DPI)

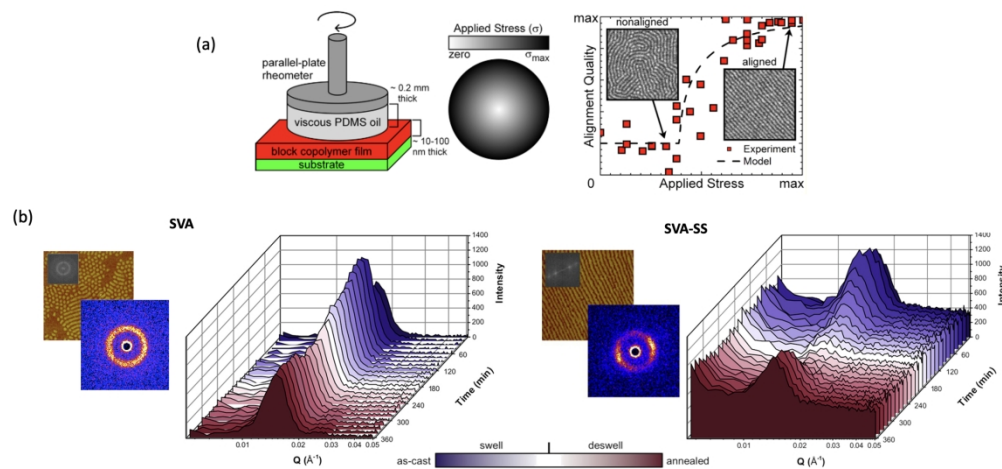


Figure 4. Studies of shear-based DSA. (a) Schematic of an experimental setup to generate shear-stress gradients, a top-down view of the applied stress gradient, and a curve of alignment quality as a function of applied shear stress for a BP system. Reproduced from ref. 63. Copyright 2015 American Chemical Society. (b) A representative SANS pattern, corresponding AFM phase image, and *in situ* SANS temporal data for poly(deuterated styrene-*b*-isoprene-*b*-deuterated styrene) over the course of swelling and deswelling for SVA (left) and SVA-SS (right). Adapted from ref. 27. Copyright 2017 American Chemical Society.

435x211mm (144 x 144 DPI)

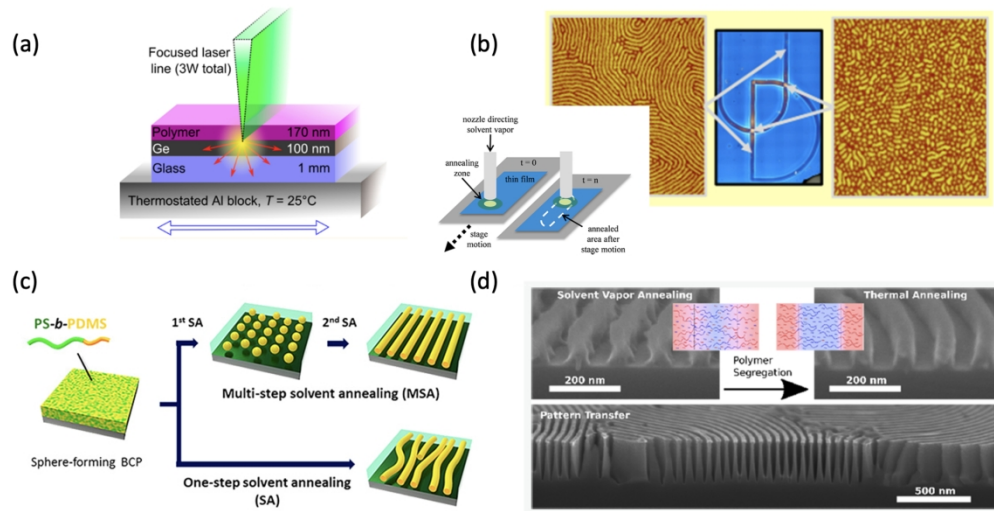


Figure 5. (a) Schematic representation of LZA: light is absorbed by a layer of germanium under a BP thin film to induce heating (yellow). The thermal profile is determined by the laser line and conduction (red arrows). Reproduced from ref. 72. Copyright 2015 American Chemical Society. (b) Illustration of the RSVA process and AFM images of an SIS thin film after a single pass of RSVA. Adapted from ref. 22. Copyright 2012 American Chemical Society. (c) A process for rapid formation of well-ordered line patterns through morphological transitions, and production of core-shell line structure using multi-step solvent annealing. Reproduced from ref. 64. Copyright 2019 American Chemical Society. (d) Annealing of UHMW BPs with low molecular weight homopolymers and SVA, and corresponding cross-sectional scanning electron microscopy images of a UHMW poly(styrene-*b*-methyl methacrylate) after self-assembly. Reproduced from ref. 65. Copyright 2020 American Chemical Society.

446x227mm (144 x 144 DPI)

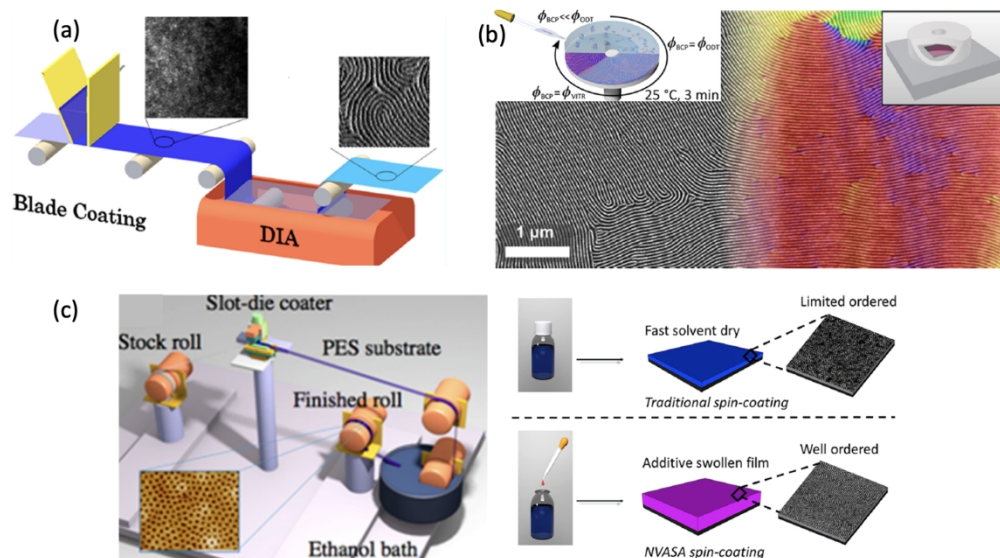


Figure 6. R2R compatible annealing methods. (a) Illustration of DIA. After a film is coated, it is submerged in a mixture of good and bad solvents (e.g., acetone and heptane, respectively, for poly(styrene-*b*-methyl methacrylate)) to anneal the BP without the use of solvent vapors. Reproduced from ref. 73. Copyright 2015 American Chemical Society. (b) Schematic representation of BP casting from a mixture of nonvolatile and volatile solvents. Scanning electron microscopy image of the resulting BP morphology with a false-color orientation map. Reproduced from ref. 61. Copyright 2020 American Chemical Society. (c) Nonvolatile solvent vapor annealing in a R2R printing process. After coating and annealing, the nonvolatile solvent is removed by submerging in an ethanol bath. The addition of a nonvolatile solvent to the casting solution results in a swollen state for the thin film after casting until the residual solvent is removed. Reproduced from ref. 92. Copyright 2019 American Chemical Society.

451x252mm (144 x 144 DPI)

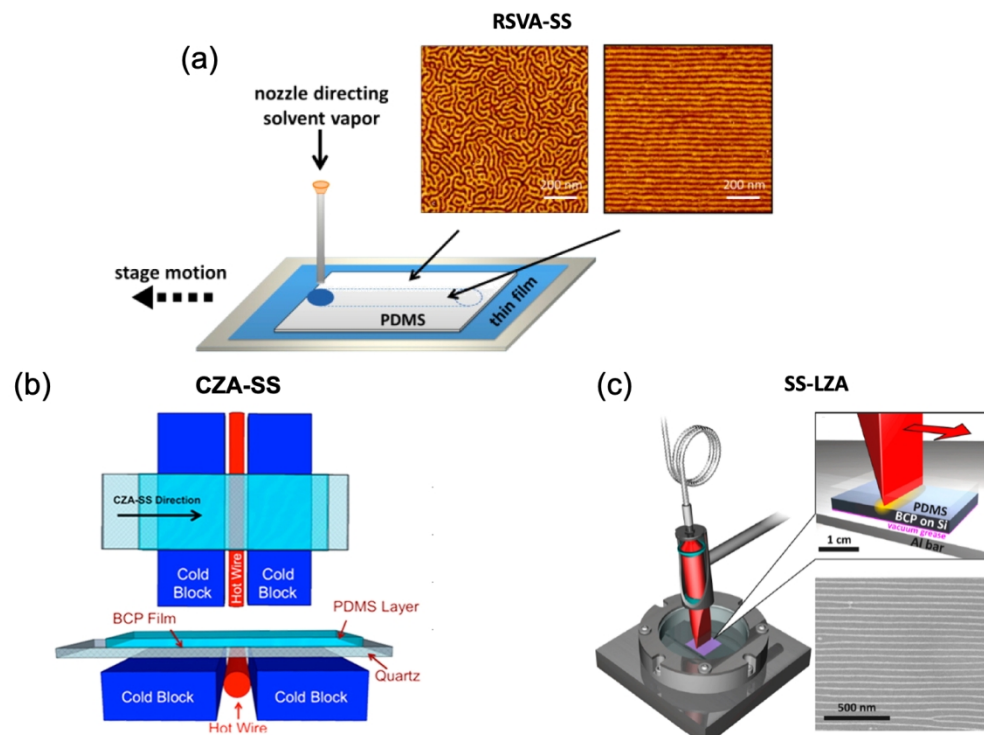
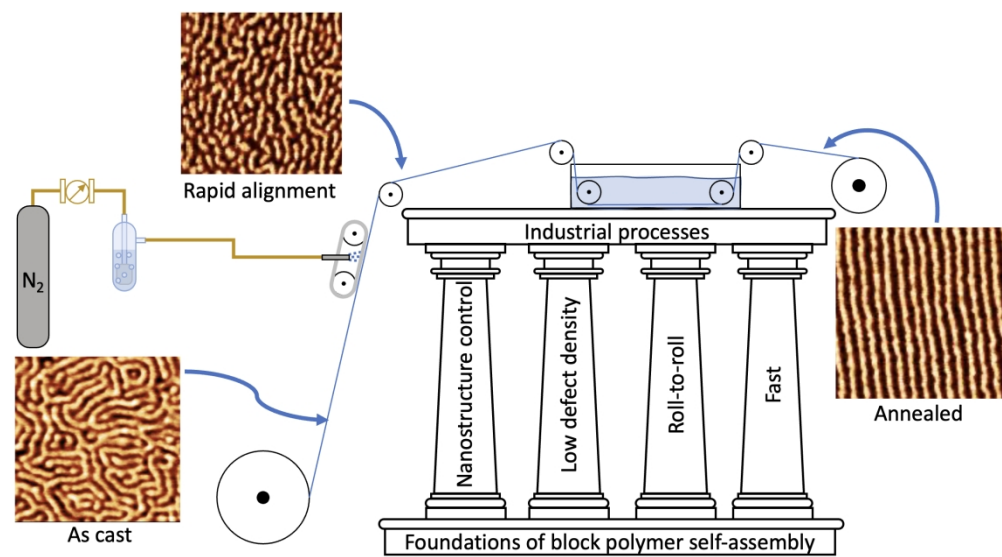


Figure 7. A comparison of different shear-based alignment methods. (a) RSVA-SS, although slower than the other techniques, has the broadest compatibility with BP systems because it uses solvent vapor as opposed to heat. Reproduced from ref. 22. Copyright 2015 American Chemical Society. (b) CZA-SS operates at moderately fast speeds and has been demonstrated with flexible substrates, but it is limited to polymer systems with $T_g \ll T_{ODT}$. Reproduced from ref. 62. Copyright 2012 American Chemical Society. (c) SS-LZA is the fastest approach demonstrated to date, but it has the same polymer constraints as CZA-SS, and the method may not be R2R compatible because the film must be placed in a vacuum chamber. Reproduced from ref. 61. Copyright 2020 American Chemical Society.

276x205mm (150 x 150 DPI)



424x232mm (144 x 144 DPI)